The Bahamas: Historical Trends and Future Climate Scenarios

Prepared by

Michael A. Taylor

Climate Studies Group, Mona

University of the West Indies

September 2016

Acknowledgements

The following persons contributed to the preparation and compilation of this report:

Michael A. Taylor

Tannecia S. Stephenson

Christina Douglas

Alrick Brown

Jayaka Campbell

Jhordanne Jones

About this Document

This report presents an assessment of literature and the results of data analyses done to characterize climate variability, trends and projections for the Bahamas, with emphasis on the islands of Great Exuma, Eleuthera and Great Abaco. The document includes (a) reviews of the current state of knowledge related to observed climate variability, trends and projections for Bahamas from authoritative literature, and (b) results from analyses of meteorological and model data.

Emphasis is placed on the key meteorological variables of rainfall and temperature, but information is also offered about historical and future hurricane frequency and intensity and sea level rise.

Table of Contents

List of Figures

List of Tables

Abbreviations

AR4	Fourth Assessment Report
AR5	Fifth Assessment Report
ASO	August-September-October
DJF	December-January-February
EOC	End of Century
ETCCDI	CCI/CLIVAR/JCOMM Expert Team on Climate Change Detection and Indices
GCM	Global Climate Model
IPCC	Intergovernmental Panel on Climate Change
JJA	June-July-August
MAM	March-April-May
MJJ	May-June-July
MSD	Mid Summer Drought
NAH	North Atlantic High
NDJ	November-December-January
PPE	Perturbed Physics Experiment
PRECIS	Providing Regional Climates for Impact Studies
RCM	Regional Climate Model
RCP	Representative Concentration Pathway
SLR	Sea Level Rise
SON	September-October-November
SRES	Special Report on Emissions Scenarios

Document Outline

This document presents historical and future climate profiles for the islands of The Bahamas from recent literature and available station, gridded and modelled data. Where possible, emphasis is placed on the islands of Great Exuma, Eleuthera and Great Abaco. Local and regional analyses of temperature, rainfall, hurricane events, and sea level rise are given. For each climate variable, the historical picture is presented followed by an analysis of their future variability under four climate scenarios. Future information is provided for four time slices representing the 2020's (2020-2029), 2030's (2030-2039), 2050's (2050-2059) and for the end-of-century (EOC) (2081-2100). Where RCM output is provided it is only up to the 2050s. The document has the following outline:

- **Section 1** provides a one-page summary describing the analysis of the report.
- **Section 2** describes the data and data sources used for developing the climate profiles and reporting on trends.
- **Section 3** briefly summarizes the process of generating future climate scenarios using global climate models (GCMs) and regional climate models (RCMs). This provides necessary context for interpreting the reported data.
- **Section 4** is a description of the historical and future surface temperature profile for locations across The Bahamas. Historical trends are gleaned from current literature and available data sets. Future rainfall trends are generated using GCM and RCM climate outputs.
- **Section 5** is a description of the historical and future rainfall profile for locations across The Bahamas. Historical trends are gleaned from current literature and available data sets. Future rainfall trends are generated using GCM and RCM climate outputs.
- **Section 6** describes historical and current trends in tropical cyclone and hurricane events in and around The Bahamas. Future trends are gleaned from current literature.
- **Section 7** presents an analysis of past and projected sea level rise in and around the Bahamas. Historical trends are calculated from mean sea level data, while projected trends are generated using the SimCLIM software.
- **Section 8** provides references.
- **Section 9** is an Appendix which provides data per grid box.

1 One-Page Summary

Historical Trend	Projection
Temperatures	
• Minimum, mean, and maximum temperatures show consistent increases with a rate of increase of ~0.013°C/year during 1901-2014. • Temperature extremes show a rate of increase of 0.1-0.3°C per decade since 1961-1990.	• GCMs project a consistent and sustained increase in mean temperatures of 0.60-0.70°C for the 2020's; 0.2-1.01°C for the 2030's; 0.83°-1.70°C for the 2050's; and 0.50°-3.06°C for the end-of-century (2081-2100). • RCMs projections indicate consistent increase in temperatures towards the 2050's, regardless of scenario, for Great Exuma, Eleuthera, and Great Abaco. • RCM projected change for Great Exuma: 1.01-1.26°C (2020's), 1.22-1.69°C (2030's), and 1.81-2.14°C (2050's). • RCM Projected change for Eleuthera: 1.12-1.27°C (2020's), 1.18-1.74°C (2030's), and 1.37-3.21°C (2050's) • RCM Projected change for Great Abaco: 1.04-1.24°C (2020's), 1.14-1.73°C (2030's), and 1.40-2.88°C (2050's)
Rainfall	
• Mean rainfall show increases with rate of increase of 0.092 mm/month for the Bahamas overall.	• Under the more moderate future scenarios (RCP2.6 and RCP4.5). The Bahamas get slightly wetter (1-2%) in the mean through to the end of the century. • Under the more severe emission scenarios The Bahamas progressively dries (1.5 to 5% drier by the end of century). • Up to mid-century variability (swings between wet and dry) seems to dominate. • Drying in the wet season (August to November) seems to contribute to the end of century drying under the more severe scenarios. • Dry season rainfall seems to slightly increase toward the end of the century under all scenarios. • RCM Projected change for Great Exuma: -8.23 to +25.96% (2020's), -10.21 to +21.10% (2030's), and -13.63 to +58.46% (2050's) • RCM Projected change for Eleuthera: -9.82 to +20.61% (2020's), -4.97 to +11.82% (2030's), and -17.87 to +43.14% (2050's) • RCM Projected change for Great Abaco: -4.27 to +20.29% (2020's), -4.97 to +11.82% (2030's), and -17.87 to +43.14% (2050's).
Hurricanes	
• Dramatic increase in frequency and duration of Atlantic hurricanes since 1995. • Increase in category 4 and 5 hurricanes; rainfall intensity, associated peak wind intensities, mean rainfall for same period. • Eleuthera seems more susceptible to hurricane influence.	• No change or slight decrease in frequency of hurricanes. • Shift toward stronger storms by the end of the century as measured by maximum wind speed increases of +2 to +11%. • +20% to +30% increase in rainfall rates for the model hurricane's inner core. Smaller increase (~10%) at radii of 200 km or larger. • An 80% increase in the frequency of Saffir-Simpson category 4 and 5 Atlantic hurricanes over the next 80 years using the A1B scenario.
Sea Levels	
• A regional rate of increase of 0.18 ± 0.01 mm/year between 1950 and 2010. • Higher rate of increase in later years: up to 3.2 mm/year between 1993 and 2010. • Caribbean Sea level changes are near the global mean.	• For the Caribbean, the combined range for projected SLR spans 0.26-0.82 m by 2100 relative to 1986-2005 levels. The range is 0.17-0.38 for 2046 – 2065. Other recent studies suggest an upper limit for the Caribbean of up to 1.5 m under RCP8.5 • For The Bahamas, projected mean SLR over all RCPs is 0.44 - 0.72 m by the end of the century. • Maximum rise is 1.12 m by the end of the century.

2 About the Data

Table 1 itemizes the datasets and data sources used to generate and calculate the historical and future trends analyzed in the coming sections.

Table 1: Data sources and usage for each variable.

Historical Data				
Temperature	Climatology	Station data	http://www.weatherbase.com	Online repository for climatological station data
	Trends	Gridded Dataset	CRU TS 3.23: fully interpolated dataset with high resolution (0.5°). Monthly gridded fields based on monthly observational data, which are calculated from daily or sub-daily data by National Meteorological Services and other external agents.	University of East Anglia Climatic Research Unit; Jones, P.D.; Harris, I. (2013). Retrieved from KNMI Climate Explorer http://climexp.knmi.nl/plot_atlas_form.py
Rainfall	Climatology	Gridded Dataset and Station Data	CRU TS 3.23: fully interpolated dataset with high resolution (0.5°). Monthly gridded fields based on monthly observational data, which are calculated from daily or sub-daily data by National Meteorological Services and other external agents.	University of East Anglia Climatic Research Unit; Jones, P.D.; Harris, I. (2013): Retrieved from KNMI Climate Explorer http://climexp.knmi.nl/plot_atlas_form.py
	Trends	Gridded Dataset	CRU TS 3.23: fully interpolated dataset with high resolution (0.5°). Monthly gridded fields based on monthly observational data, which are calculated from daily or sub-daily data by National Meteorological Services and other external agents.	University of East Anglia Climatic Research Unit; Jones, P.D.; Harris, I. (2013): Retrieved from KNMI Climate Explorer http://climexp.knmi.nl/plot_atlas_form.py
Extremes	Trends Climatology	Gridded Dataset and Station Data	Expert Team on Climate Change Detection and Indices (ETCCDI) Extremes Indices computed from daily station data and/or using global climate models participating in CMIP3	For further information: http://etccdi.pacificclimate.org/index.shtml
Hurricanes	Trends		NCEP-NCAR HURDAT 'Best-Track' Dataset	Retrieved from http://www.aoml.noaa.gov/hrd/data_sub/re_anal.html

Table 1 continued.

Sea Level Rise	Trends	Station Data	Permanent Service for Mean Sea Level (PSMSL)	Retrieved from http://www.psmsl.org/
Future Data				
Temperature and Rainfall	GCM Data	Gridded Dataset	CMIP5 (IPCC AR5 Atlas subset) This is the dataset used in the IPCC WG1 AR5 Annex I "Atlas". Only a single realization from each of over 20 models is used. All models are weighed equally, where model realizations differing only in model parameter settings are treated as different models.	Retrieved from KNMI Climate Explorer http://climexp.knmi.nl/plot_atlas_form.py
Extremes	GCM and RCM Data	Gridded Dataset	Expert Team on Climate Change Detection and Indices (ETCCDI) Extremes Indices computed from CMIP3 global climate models and PRECIS Perturbed Physics experiments performed for the Caribbean.	For further information: http://etccdi.pacificclimate.org/index.shtml
Sea Levels	GCM Data	Gridded Dataset	CMIP5 model data accessed through SIMCLIM	http://www.climsystems.com/simclim/
Hurricanes			As reported in literature	Various sources

Additional information on the model data is provided in Section 3.

Future downscaled data from the RCM are provided for 25 km square grid boxes. The grid boxes covering Great Exuma, Eleuthera and Great Abaco islands are shown in Figure 1. The coordinates for each grid box are provided in Table 2. Projection summaries by grid box may be found in the Appendices.

Table 2: Select islands and associated grid box coordinates.

Isle	Grid Box No.	Longitude (^oW)	Latitude (^oN)
Great Exuma	1	75.54	23.34
	2	75.76	23.56
	3	75.98	23.56
Eleuthera	4	76.20	24.66
	5	76.20	24.88
	6	76.20	25.10
	7	76.20	25.32
	8	76.42	25.32
	9	76.64	25.32
	10	76.64	25.54
Great Abaco	11	77.30	25.98
	12	77.08	26.20
	13	77.30	26.20
	14	77.08	26.42
	15	77.30	26.42
	16	77.08	26.64
	17	77.30	26.64
	18	77.52	26.86
	19	77.74	26.86
	20	77.96	26.86

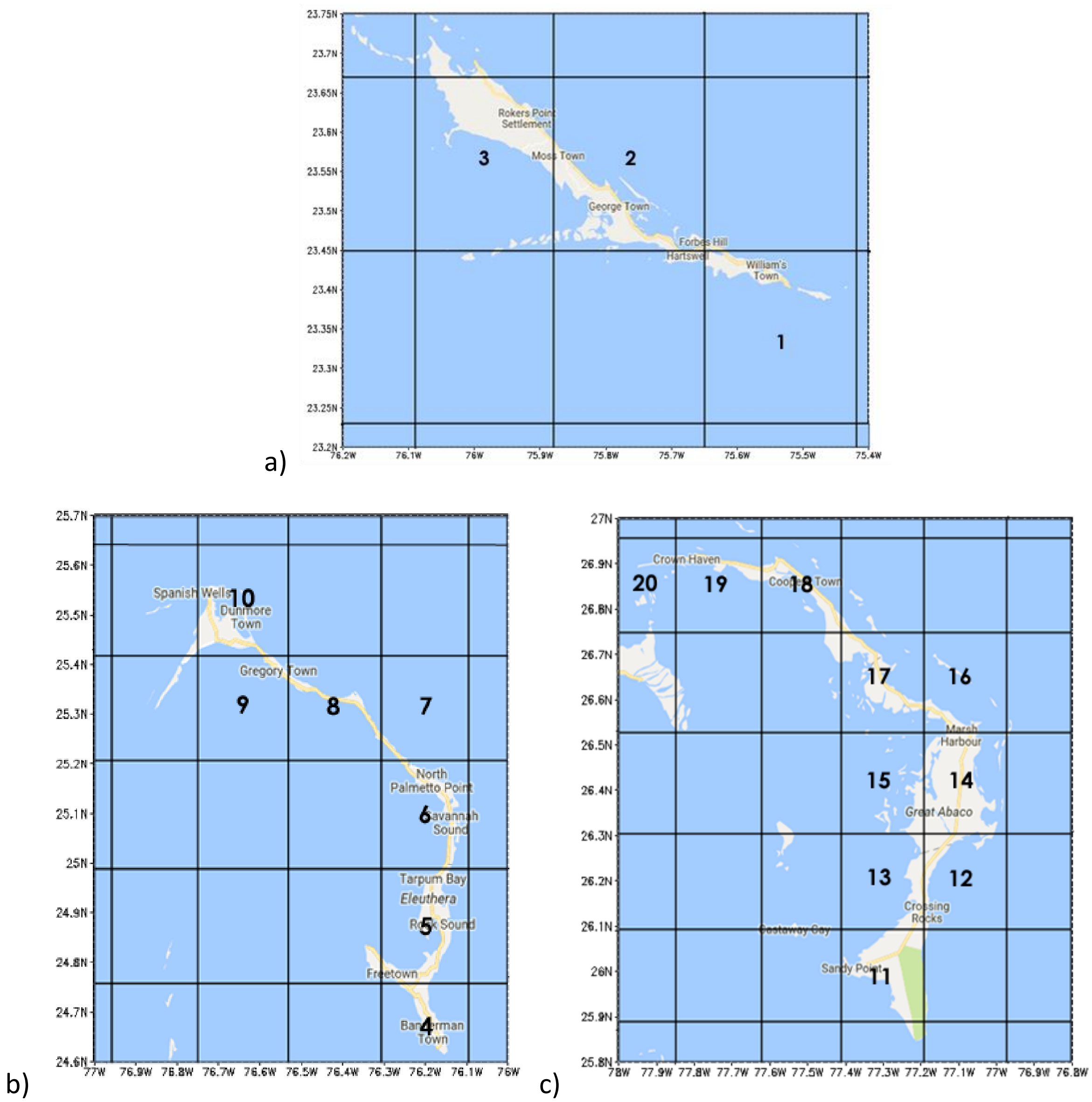

Figure 1: Diagram highlighting grid boxes used to analyze climatic trends over a) Great Exuma, b) Eleuthera, and c) Great Abaco.

3 Obtaining Future Climate Projections

3.1 Global Climate Models (GCMs)

Global climate models, also referred to as general circulation models, are mathematical representations of the physical and dynamical processes in the atmosphere, ocean, cryosphere and land surfaces. Their physical consistency and skill at representing current and past climates make them useful for simulating future climates under differing scenarios of increasing greenhouse gas concentrations (discussed further below) and aerosol forcings.

Projections for minimum, mean, and maximum near-surface temperatures and precipitation are generated for the Bahamas using a subset of models developed under the Coupled Model Intercomparison Project Phase 5 (CMIP5). Phase 5 of the CMIP initiative is a recent undertaking by the Intergovernmental Panel on Climate Change (IPCC) to provide higher resolution projections for assessing regional climate impacts. The initiative is documented in the IPCC's Fifth Assessment Report (AR5) (IPCC 2013). The GCM projections will provide a context within which sub-country scale projections may be interpreted and compared. Projections are generated for the 2020's (2020-2029), 2030's (2030-2039), 2050's (2050-2059), and the end-of-century (2081-2100). Future climate outputs were extracted under the four Representative Concentration Pathways (RCPs), further discussed in Section 3.3. These projections are presented in the form of figures and summary tables.

3.2 Regional Climate Models (RCMs)

An inherent drawback of the GCMs, however, is their coarse resolution relative to the scale of required information. The size of the islands of the Bahamas versus the grid spacing of the GCMs on which data are reported means that they are represented by at most a few grid boxes, and there is a need for *downscaling* techniques to provide more detailed information on a sub-country level. The additional information which the downscaling techniques provide do not however devalue the information provided by the GCMs especially since (1) to a large extent the climate of the Bahamas is driven by large-scale phenomenon (2) the downscaling techniques themselves are driven by the GCM outputs, and (3) at present the GCMs are the best source of future information on some phenomena e.g. hurricanes.

Statistical and *dynamical* downscaling are the two methods normally applied to achieve finer resolution information. It is the results of *dynamical* downscaling that are reported on in this study. *Dynamical* downscaling employs a regional climate model (RCM) driven at its boundaries by the outputs of the GCMs. Like GCMs, the RCMs rely on mathematical representations of the

physical processes, but are restricted to a much smaller geographical domain (the Caribbean in this case). The restriction enables the production of data of much higher resolution (typically < 100 km). Available RCM data for The Bahamas were obtained from the PRECIS (Providing Regional Climates for Impact Studies) model (Taylor et al. 2013) run at a resolution of 25 km.

The PRECIS RCM was developed by the Hadley centre (UK) to facilitate the generation of high-resolution climate change information for as many regions of the world as possible. PRECIS is made freely available to groups of developing countries in order that they may develop climate change scenarios at national centres of excellence, simultaneously building capacity and drawing on local climatological expertise. http://www.metoffice.gov.uk/precis/intro. PRECIS is a hydrostatic primitive equations grid point model. It contains 19 levels in the vertical and has horizontal resolutions of 0.44°x0.44° (~50 km) and 0.22°x0.22° (~25 km). Initial and lateral boundary forcing are taken from reanalysis or from outputs of GCMs. The sea surface temperatures (SSTs) and sea-ice fractions surface boundary conditions are from a combination of monthly HadISST1 dataset and weekly NCEP observed datasets. Observed values of greenhouse gases are also fed into the model. PRECIS utilizes a relaxation technique across a four point buffer zone at each vertical level. Dynamical flow, the atmospheric sulphur cycle, clouds and precipitation, radiative processes, the land surface and the deep soil are also described in the model. A full description of the model's physics is found in Jones et al. (2004).

Validation of the PRECIS Model for the Caribbean is offered in a number of papers including Campbell et al. (2011) and Taylor et al. (2013). Campbell et al. (2011) '*compared PRECIS's modeled patterns of temperature and precipitation with reanalysis datasets and available observations. They showed the mean Caribbean climatologies to be generally captured by the model, with the relative timing of temperature and precipitation maxima and minima being reproduced. This included the model's reproduction of the Caribbean midsummer rainfall minimum, which is a significant feature of many of the larger Caribbean islands. There was, however, also a general underestimation of rainfall amounts across the main Caribbean basin during the wet season and a simulation using temperatures that were too warm over the Caribbean islands but too cold over Central America and northern South America' (Taylor et al. 2013).*

The PRECIS RCM results used in this study are derived from PRECIS driven perturbed physics experiments (PPE). The PPE's were created using the A1B SRES scenario (see following section on scenarios) and provide an alternative to using several driving GCM boundary conditions (McSweeney et al 2012). PRECIS PPEs comprise a 17 member ensemble (HadCM3Q0-Q16), however for the purposes of this study a subset of 6 representative of the overall range of key climate features were used. The 6 used are the ensemble members Q0, Q3, Q4, Q10, Q11 and Q14.

Figure 1 shows the spatial representation of the islands of Great Exuma, Eleuthera, and Great Abaco in the PRECIS RCM. Ensuing results will seek to detail temperature (mean, maximum and minimum) and rainfall changes associated with the grid boxes noted in Table 2. For each of these variables the average of the 6 perturbations is presented as well as the minimum and maximum associated change on the seasonal and annual time scales.

3.3 Emissions Scenarios

The GCMs and RCM were run using either the Special Report Emission Scenarios (SRES) (Nakićenović et al. 2000) or Representative Concentration Pathways (RCPs).

Each SRES scenario is a plausible storyline of how a future world will look. The scenarios explore pathways of future greenhouse gas emissions, derived from self-consistent sets of assumptions about energy use, population growth, economic development, and other factors. They however explicitly exclude any global policy to reduce emissions to avoid climate change. Scenarios are grouped into families according to the similarities in their storylines as shown in Figure 2.

The RCM results presented in the following section are for the A1B scenario using the Perturbed Physics Ensembles (PPE) approach. The A1B scenario is characterized by an increase in carbon dioxide emissions through mid-century followed by a decrease (Figure 3). A1B is often seen as a compromise between the A2 (high emissions) and B2 (lower emissions) scenarios.

In the IPCC Fifth Assessment Report (AR5), outcomes of climate simulations use new scenarios (some of which include implied policy actions to achieve mitigation) referred to as "Representative Concentration Pathways" (RCPs) (Figure 4). These RCPs represent a larger set of mitigation scenarios and were selected to have different targets in terms of radiative forcing of the atmosphere at 2100 (about 2.6, 4.5, 6.0 and 8.5 W/m^2). They are defined by their total radiative forcing (cumulative measure of human emissions of greenhouse gases from all sources expressed in Watts per square metre) pathway and level by 2100. i.e. RCP2.6. RCP4.5, RCP6.0 and RCP8.5. The scenarios should be considered plausible and illustrative, and do not have probabilities attached to them.

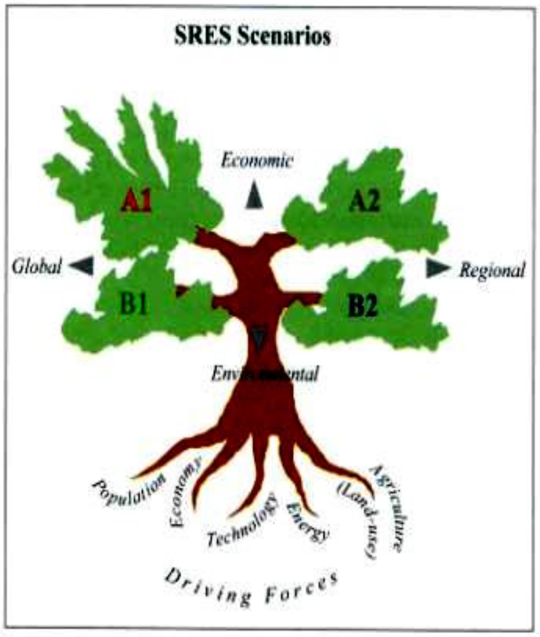

Figure 2: Special Report on Emission Scenarios (SRES) schematic and storyline summary (Nakicenovic et al. 2000).

- **A1** storyline and scenario family: a future world of very rapid economic growth, global population that peaks in mid-century and declines thereafter, and rapid introduction of new and more efficient technologies.
- **A2** storyline and scenario family: a very heterogeneous world with continuously increasing global population and regionally oriented economic growth that is more fragmented and slower than in other storylines.
- **B1** storyline and scenario family: a convergent world with the same global population as in the A1 storyline but with rapid changes in economic structures toward a service and information economy, with reductions in material intensity, and the introduction of clean and resource-efficient technologies.
- **B2** storyline and scenario family: a world in which the emphasis is on local solutions to economic, social, and environmental sustainability, with continuously increasing population (lower than A2) and intermediate economic development.

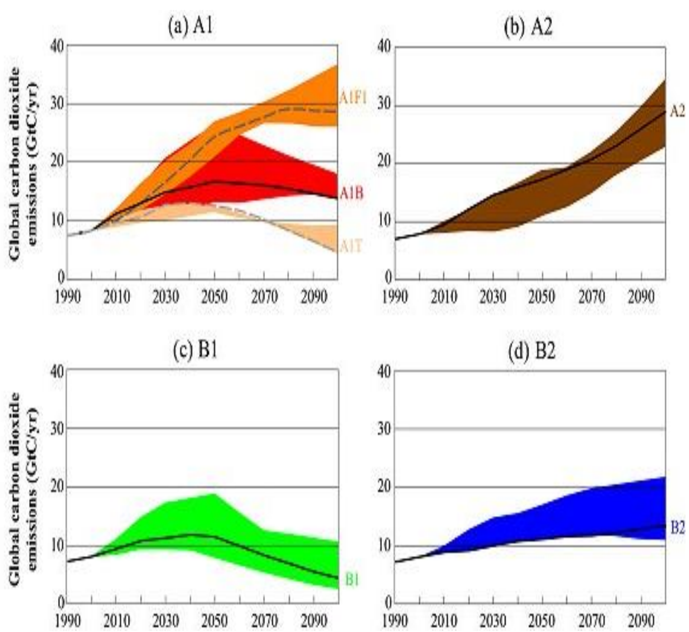

Figure 3: Total global annual CO_2 emissions from all sources (energy, industry, and land-use change) from 1990 to 2100 (in gigatonnes of carbon (GtC/yr) for the families and six SRES scenario groups (Nakicenovic et al. 2000).

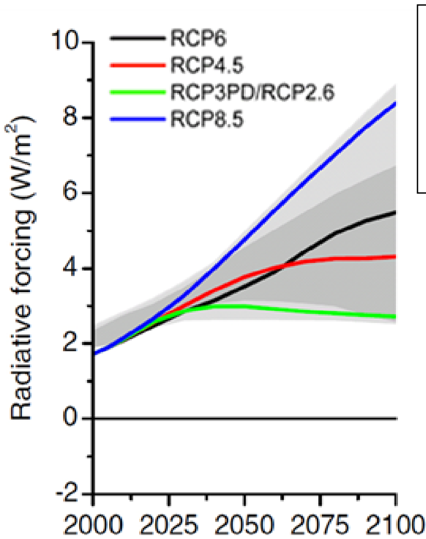

Figure 4: Radiative forcing of the Representative Concentration Pathways. Taken from van Vuuren et al. (2011). The light grey area captures 98% of the range in previous IAM scenarios, and dark grey represents 90% of the range.

RCP	**Comments**	**Radiative Forcing Behaviour**
RCP2.6	Lowest	Peaks at 3 Wm^{-2} and then declines to approximately 2.6 Wm^{-2}
RCP4.5	Medium-low	Stabilization at 4.5 Wm^{-2}
RCP6	Medium-high	Stabilization at 6 Wm^{-2}
RCP8.5	Highest	RF of 8.5 Wm^{-2} by 2100 but implies rising RF beyond 2100

It is to be noted that whereas the SRES scenarios resulted from specific socio-economic scenarios from storylines about future demographic and economic development, regionalization, energy production and use, technology, agriculture, forestry and land use (IPCC, 2000), the RCPs are new scenarios that specify concentrations and corresponding emissions, but not directly based on socio-economic storylines like the SRES scenarios. These four RCPs include one mitigation scenario leading to a very low forcing level (RCP2.6), two stabilization scenarios (RCP4.5 and RCP6), and one scenario with very high greenhouse gas emissions (RCP8.5). The RCPs can thus represent a range of 21st century climate policies, as compared with the no-climate policy of the Special Report on Emissions Scenarios (SRES) used in the Third Assessment Report and the Fourth Assessment Report (Figures 2 and 3). It is to be noted that many do not believe RCP2.6 is feasible without considerable and concerted global action.

The GCM results presented in the following section are for the four RCPs.

3.4 Perturbed Physics

Perturbed Physics Experiments (PPEs) are designed by varying uncertain parameters in the model's representation of important physical and dynamical processes. PPEs are used to capture some major sources of modelling uncertainty by running each member using identical climate forcings. It provides an alternative to using GCMs developed at different modelling

centres around the world (e.g. a multi-model ensemble, MME), like those in the CMIPs (Coupled Model Intercomparison Projects). The Hadley Centre's PPE includes 17 members which are formulated to systematically sample parameter uncertainties under the *A1B emissions scenario* – this is referred to as the QUMP (Quantifying Uncertainties in Model Projections) ensemble. The QUMP ensemble was designed for use in the UK's own climate projections and is described in detail in the UKCP report available online at http://ukclimateprojections.defra.gov.uk/content/view/944/500/. Globally, and for many regions and variables, the range of climate futures projected by the QUMP PPE is equivalent or greater than those based on the CMIP MME. The PPE systematically samples the parameter uncertainties, exploring a wider range of possible variation in the formulation of a single model, leading to a wider range of physically plausible future climate outcomes than the MME. It is important to remember that PPE (similarly for MME) does not account for all of the sources of model uncertainty. [1]

As noted previously, the following 6 QUMP experiments were evaluated: Q0, Q3, Q4, Q10, Q11, and Q14. All were run at 25 km and from 1960 through 2100. For each experiment the deviation of a future decade e.g. 2020s, 2030s from the experiments baseline (1961-1990) were determined. This gave an ensemble of 6 future changes for each decade. The ensemble results are summarised and presented in Tables for the 2020s and 2030s as requested.

3.5 Presenting the Future RCM Data

Future change data from the RCMs are provided for five variables. For four of the five variables the data are provided as absolute change. These variables are: minimum temperature (^{o}C), maximum temperature (^{o}C), and mean temperature (^{o}C). Percentage change is provided for precipitation. Data is averaged for over three month seasons: November-January (NDJ), February-April (FMA), May-July (MJJ) and August–October (ASO), roughly consistent with the Caribbean dry season and wet season (Taylor et al. 2002). The mean annual change is also given. The change for each variable and for each period is calculated for the 2020s and 2030s for each member of the ensemble. The minimum, maximum and mean values of the 6 member ensemble are provided.

[1] Portions of the narrative are adapted from narrative on the PRECIS webpage http://www.metoffice.gov.uk/precis/qump

4 Temperature

4.1 Climatology

Temperatures across the Bahamas follow the general pattern typical of the Caribbean region. Most Caribbean islands register a peak in temperatures in the July-October season.

Figure 5 below highlights the trend at Nassau, for both maximum and minimum temperatures for 1961-2011. The plots similarly show a general increase in temperatures peaking in July-August. Chenoweth (1998) also documented variations in homogenized daily temperature values from 1811 to 1845 for a weather station at Nassau. While the 1961-2011 climatology in minimum temperatures does not seem to differ significantly from the 1811-1845 climatology, there is a more significant difference in the climatologies of maximum temperatures – the current period being warmer than the past. The difference is most notable across July-October, suggesting a warming of the summer period. The CRU data similarly indicates a warming in more recent times (Figure 6).

Because of its more northerly location in the Caribbean, minimum temperatures in the Bahamas, particularly at the start of the year, can fall below 20°C. This reflects the influence of the passage of cold fronts.

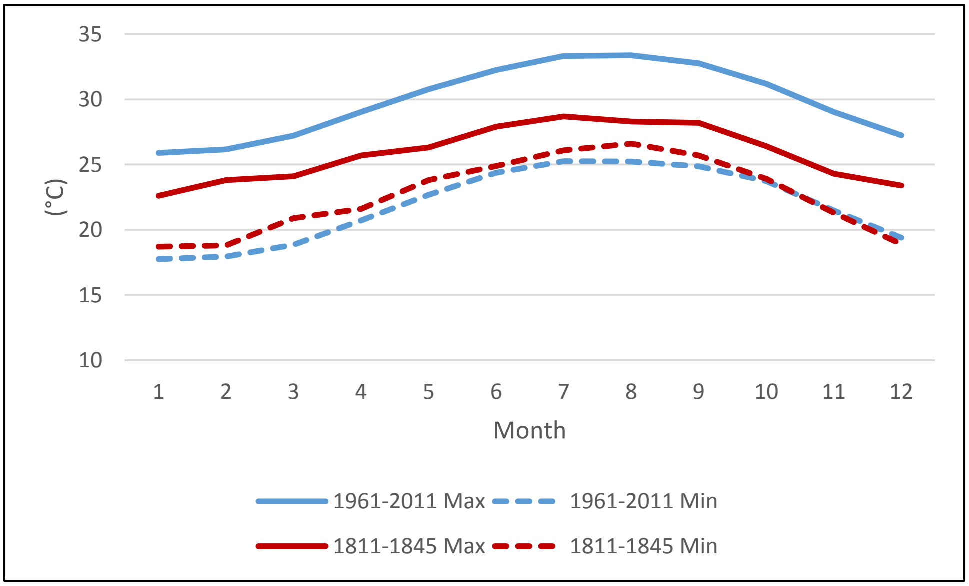

Figure 5: The 1961-2011 climatologies for minimum and maximum temperatures at Nassau, Bahamas, compared with 1811-1845 climatologies of minimum and maximum temperatures for the same station. Data Source: RClimDex, Chenoweth (1998).

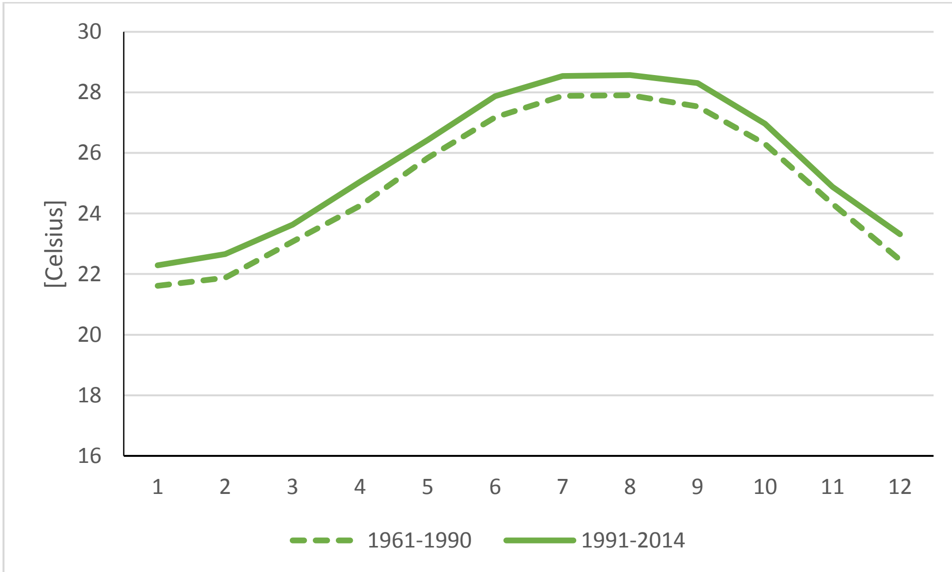

Figure 6: Comparison of the 1961-1990 mean temperature climatology and the more recent 1991-2014 temperature climatology. Data Source: CRU TS3.23.

4.2 Trends and Variability

Temperatures over the past few decades display a distinct increasing trend across the Caribbean region. This is true for the Bahamas for minimum, maximum and mean temperatures (Figure 7). Time series generated from the CRU TS3.23 dataset (Figure 7) indicate a rate of increase of mean temperatures of approximately 0.013°C per year (or 0.13 degrees per decade) for the period 1901-2014. The increase is comparable with that for the rest of the Caribbean For example, Antuña et al. (2015) observe a rate of increase of 1.32°± 0.82°C per century (0.0132°C per year) for the Eastern Caribbean and 1.08° ± 0.71°C per century (0.0108°C per year) for the wider Caribbean from 1906 to 2005.

Trends in the minimum and maximum temperatures for The Bahamas, show a similar rate of increase over the 113-year period analysed (Figure 7). This is in contrast to the rest of the Caribbean which generally shows a slightly larger trend for minimum temperatures than for maximum temperatures (Stephenson et al. 2014).

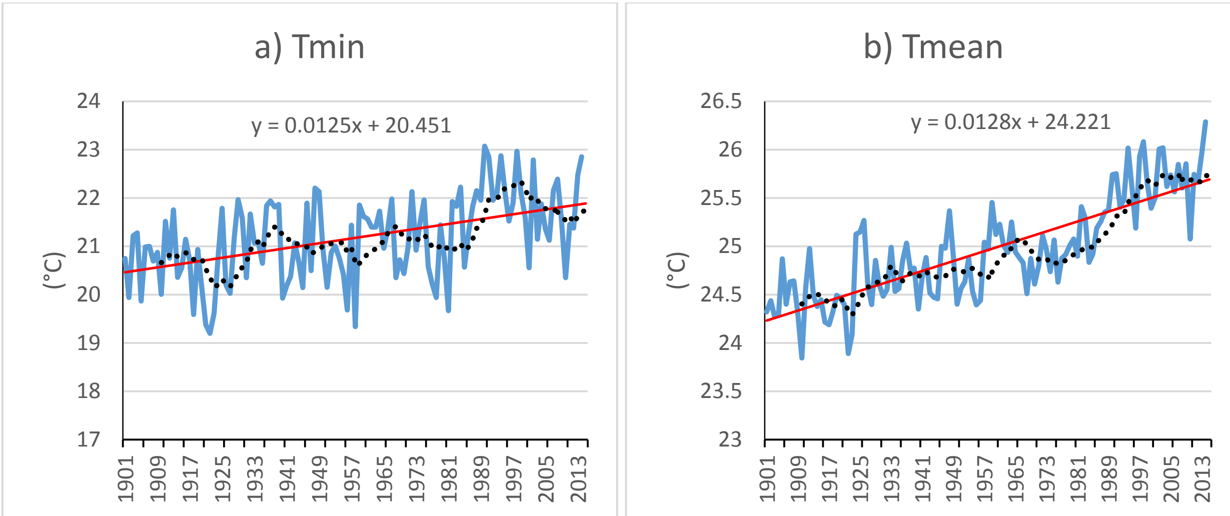

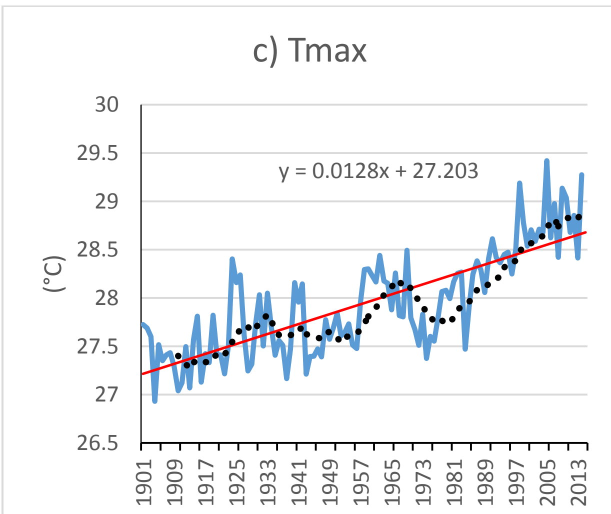

Figure 7: The annual a) minimum, b) mean, and c) maximum temperatures for The Bahamas for 1901-2014. The linear trend is indicated in red. The black dotted line represents the 10-year moving average. Data Source: CRU TS3.23.

The observed variability in Caribbean climate can often be accounted for by three main time scales: trends, decadal variability and inter-annual variability. The ‘trend’ time scale loosely represents the variation in temperatures due to anthropogenic influences, and accounts for 54% of the variability in Caribbean temperature records. That is, the anthropogenic signal is the strongest driver of variability in the historical Caribbean temperature records. In addition to long term linear trends, however, large-scale atmospheric variability also plays a significant role in driving the climate of the Caribbean (Giannini et al. 2000; Giannini et al. 2001; Taylor et al. 2002; Gamble et al. 2008; Klotzbach 2011; Maldonado et al. 2015). Two major drivers of variability in Caribbean surface temperatures on the decadal and inter-annual (year-to-year) scales respectively are the Atlantic Multidecadal Oscillation (AMO) and the El Niño Southern Oscillation (ENSO). The decadal and inter-annual scales represent the natural variability of region’s temperatures, and account for approximately 14% and 30%, respectively.

Figure 8 shows that for the region near and around The Bahamas, 65% of the variability in the mean surface temperature is due to the linear trend with decadal and inter-annual variability accounting for 9% and 24%, respectively. Antuña et al. (2015) suggest that the AMO is a major driver of the decadal variations in temperature, while ENSO is the primary driver of inter-annual temperature variations.

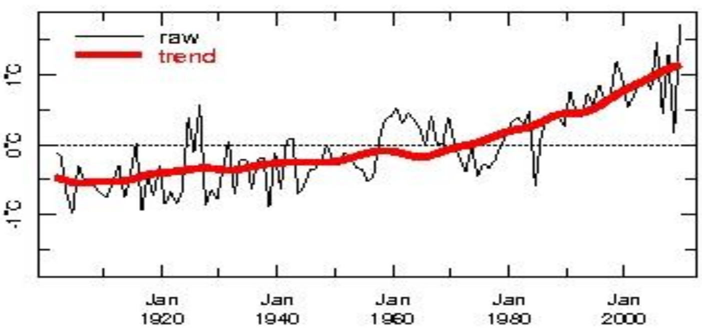

Trend	65%
Decadal	9%
Inter-annual	24%

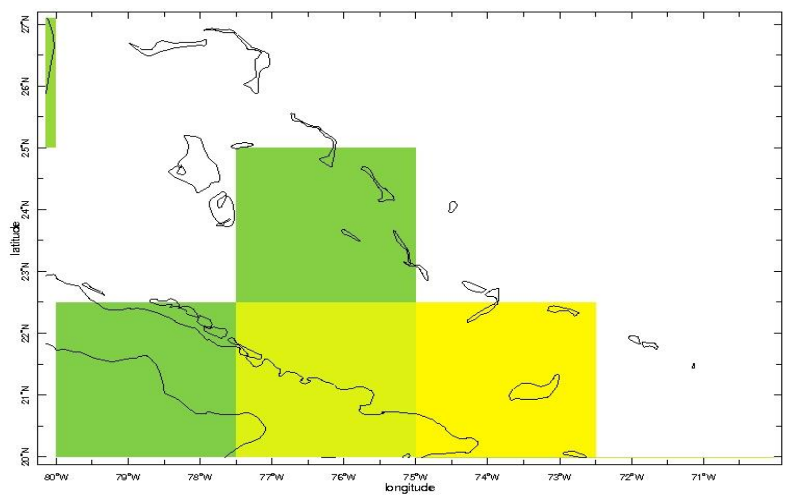

Figure 8: (a) Average July-October temperature anomalies over the Bahamas from the late 1800s with trend line imposed. Box inset: Percentage of variance explained by trend line, decadal variations (> 10 years), and inter-annual (year-to-year) variations. (b) Percentage variance in July-October temperature anomalies (from late 1800s) accounted for by the 'global warming' trend line for grid boxes over the Bahamas. Data source: CRU TS3.10. Acknowledgements: IRI Map Room.

4.3 Temperature Extremes

4.3.1 Caribbean

Stephenson et al. (2014) analyzed trends in temperature and precipitation extremes for various stations across the Caribbean using homogenized data sets. From Figure 9, maximum and minimum temperature extremes in and around the Bahamas show a general warming trend with a rate of increase of 0.1-0.3°C per decade for the period 1961-2010. This is similar to what was previously reported. There is a slight reduction in the diurnal temperature range (DTR), defined as the annual mean difference between maximum and minimum temperatures, over the same period.

An increasing trend is also evident for other variables characterizing extremes in temperature (Figure 10). TX90p (the percentage of days of the warmest maximum temperatures) and TN90p (the percentage days of the warmest minimum temperatures) have both shown statistically significant increases indicating more warm days and nights per year. TX10p (the percentage of days of the coolest maximum temperatures) and TN10p (the percentage of days of the coolest minimum temperatures) have correspondingly decreased indicating the trend toward fewer cool days and cool nights per year. Stephenson et al. (2014) indicates that the number of cool days (cool nights) across the Caribbean region decline by 1.8% (2.6%) over the 1961-2010 period.

4.3.2 Extremes over Nassau, Bahamas

Table 3 shows the 1981-2001 seasonal average number of warm days, warm nights, cool days, and cool nights for Nassau, Bahamas. During the DJF and MAM seasons, the number of cool days and cool nights are generally more than the number of warm days and nights. The number of warm days and nights, however, total more than the cool days and nights during the seasons of JJA and SON. In general, historical numbers indicate that the number of warm days and cool nights experienced in Nassau are comparable.

Trends across the 1981-2001 period indicate a general decline in the number of cool days (1.53 less days per year) and cool nights (0.19 less days per year) over Nassau. The number of warm days and nights ae also increasing with a trend of 1.37 more days per year and 1.66 more days per year respectively.

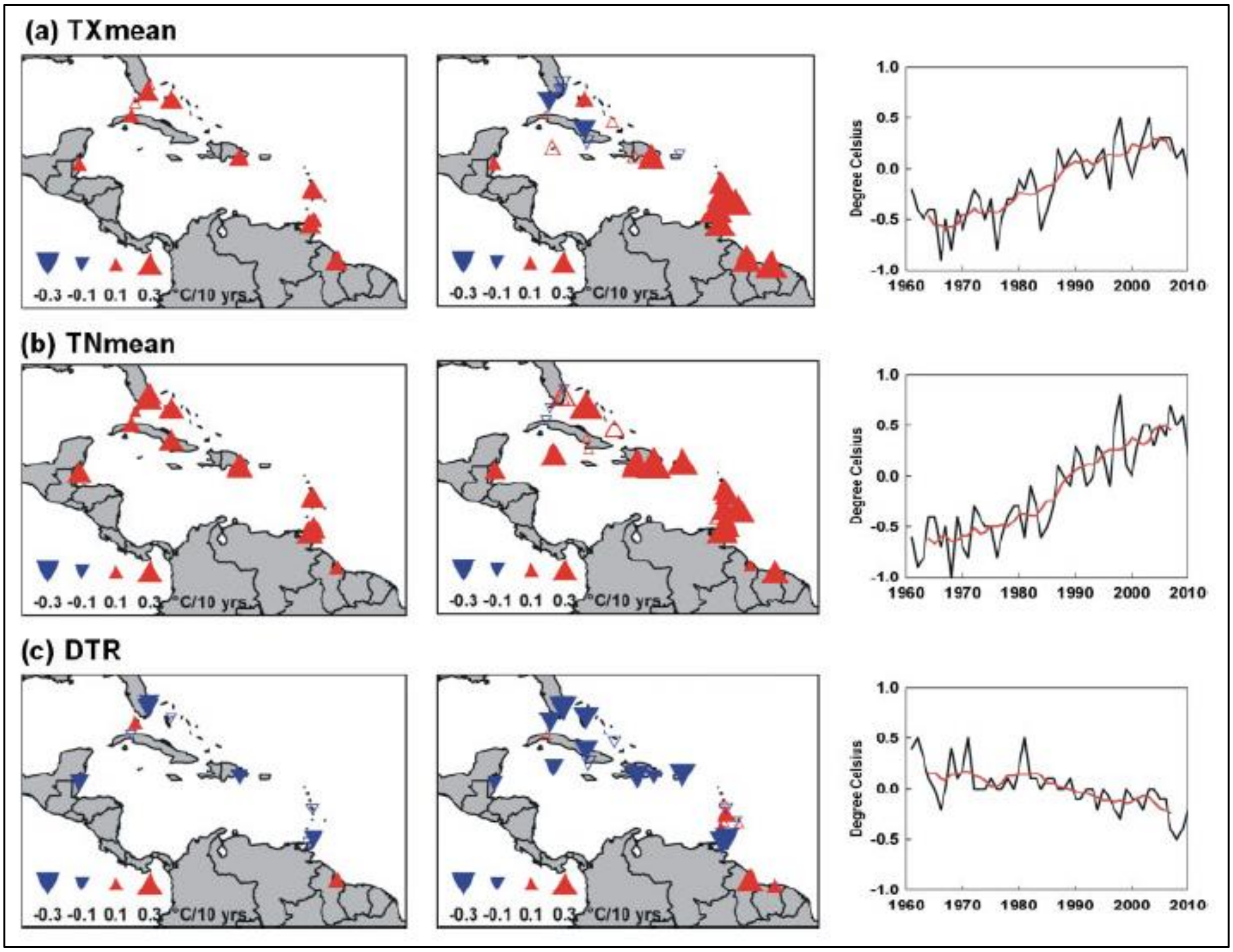

Figure 9: Trends in (a) maximum temperature (TXmean), (b) minimum temperature (TNmean) and (c) diurnal temperature range (DTR). Left panels show the trends for 1961-2010; middle panels show the trends for 1986-2010; and right panels present the time series for area-averaged anomalies for 1961-2010 relative to a 1981-2000 climatology. Upward (downward) pointing triangles indicate positive (negative) trends. Solid triangles correspond to trends significant at the 5% level. The size of the triangle is proportional to the magnitude of the trend. Red colour indicates warming, blue indicates cooling trends in (a) and (b); blue colour indicates that the daily minimum is increasing more than the daily maximum in (c). The red line in the right panels is a 7-point running mean. Adapted from Stephenson et al. (2014).

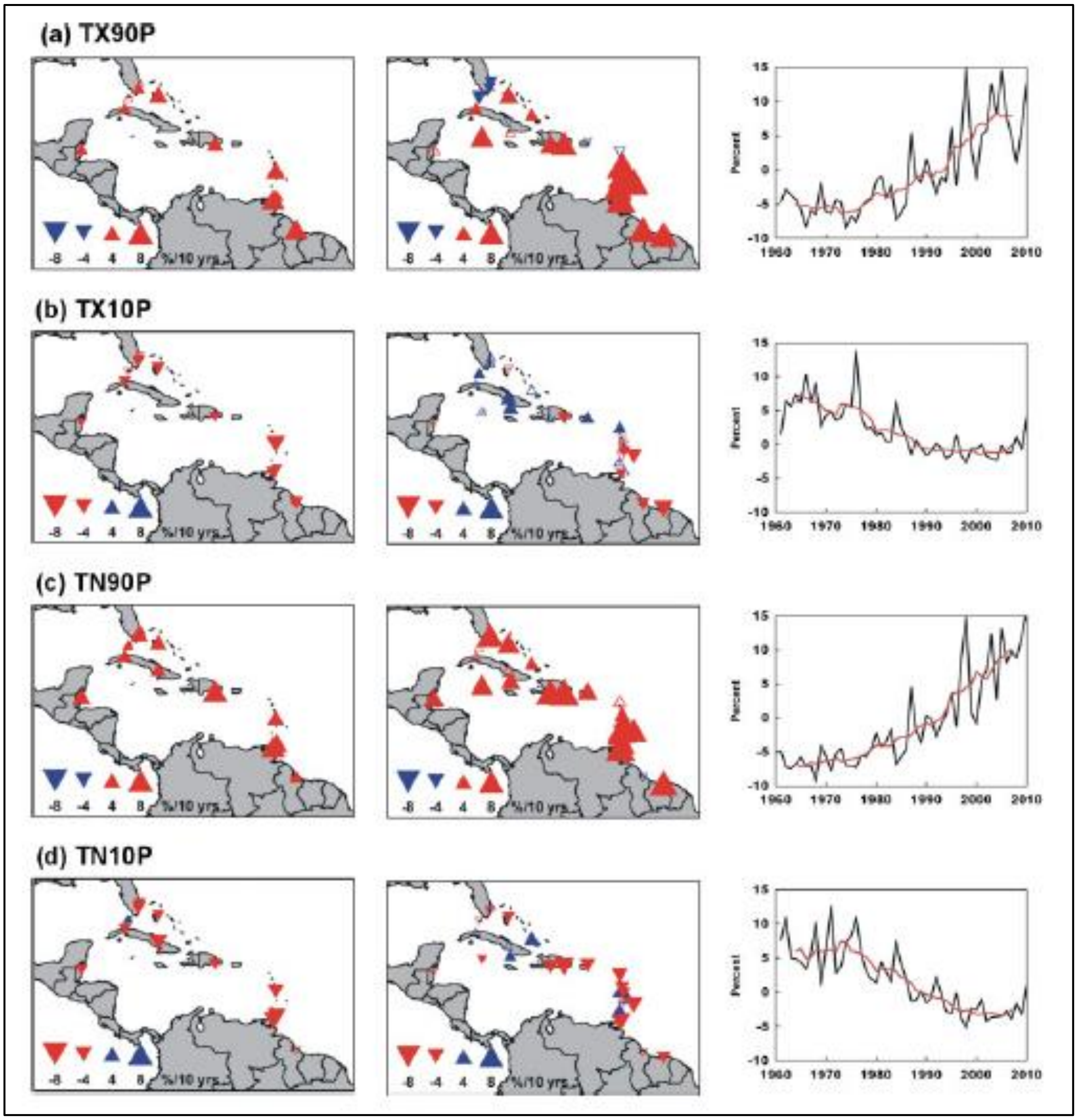

Figure 10: Same as Figure 9 above but for (a) TX90p, (b) TX10p, (c) TN90p, and (d) TN10p. Red colour indicates warming, blue colour indicates cooling trends. Adapted from Stephenson et al. (2014).

Table 3: Seasonal and annual numbers of warm days, warm nights, cool days, and cool nights over the period 1981-2001 for Nassau, Bahamas. The trends in temperature extremes are shown across 1981-2001.

	Warm Days	Warm Nights	Cool Days	Cool Nights
DJF	0	0	507	457
MAM	24	12	143	238
JJA	562	371	0	4
SON	152	159	14	30
Annual	738	542	664	729
Trend across 1981-2001 (yr^{-1})	**+1.37**	**+1.66**	**-1.53**	**-0.19**

4.4 Projections

4.4.1 GCM Projections

Ensemble-averaged projections of minimum, mean, and maximum temperatures for the GCM grid boxes covering Great Exuma, Great Abaco, and Eleuthera are summarized in Table 2. The changes shown in this table span all RCPs. The GCM projections indicate a steady increase in temperature changes towards the end of the century.

Tables 4-6 further show the projected temperatures with each RCP but for The Bahamas as a whole. A graphical representation of the projected temperature changes relative to a 1986-2005 baseline for each of the RCPs is given in Figure 11. Projections are compared to the GCMs' historical run (shown in black).

Table 4: Mean annual absolute temperature change for The Bahamas with respect to 1986-2005. Temperature change shown for four RCP scenarios. Data Source: AR5 CMIP5 subset, KNMI Climate Change Atlas.

	Tmean											
	2020's			2030's			2050's			EOC		
Averaged over	2020-2029			2030-2039			2050-2059			2081-2100		
	min	mean	max	min	mean	max	min	mean	max	min	mean	max
rcp2.6	0.49	0.62	0.67	0.61	0.70	0.77	0.80	0.84	0.87	0.76	0.80	0.86
rcp4.5	0.52	0.62	0.75	0.71	0.81	0.95	1.10	1.16	1.23	1.45	1.52	1.61
rcp6.0	0.39	0.54	0.64	0.63	0.70	0.83	0.95	1.07	1.16	1.64	1.84	2.02
rcp8.5	0.55	0.69	0.81	0.77	0.94	1.12	1.51	1.65	1.84	2.66	3.04	3.40
Range of mean	0.54 – 0.69			0.70 – 0.94			0.84 – 1.65			0.80 – 1.65		

Table 5: Annual minimum absolute temperature change for The Bahamas with respect to 1986-2005. Temperature change shown for four RCP scenarios. Data Source: AR5 CMIP5 subset, KNMI Climate Change Atlas.

	Tmin											
	2020's			2030's			2050's			EOC		
Averaged over	2020-2029			2030-2039			2050-2059			2081-2100		
	min	mean	max	min	mean	max	min	mean	max	min	mean	max
rcp2.6	0.51	0.62	0.69	0.58	0.70	0.80	0.80	0.84	0.88	-0.09	0.07	0.20
rcp4.5	0.53	0.62	0.75	0.70	0.81	0.96	1.08	1.17	1.25	-0.11	0.03	1.64
rcp6.0	0.37	0.53	0.61	0.61	0.69	0.82	0.94	1.04	1.12	1.64	1.83	2.02
rcp8.5	0.54	0.69	0.84	0.78	0.95	1.12	1.54	1.68	1.87	2.71	3.07	3.43
Range of mean	0.53 – 0.69			0.69 – 0.95			0.84 – 1.68			0.03 – 3.07		

Table 6: Annual maximum absolute temperature change for The Bahamas with respect to 1986-2005. Temperature change shown for four RCP scenarios. Data Source: AR5 CMIP5 subset, KNMI Climate Change Atlas.

	Tmax											
Centered on	2025			2035			2055			EOC		
Averaged over	2016-2035			2026-2045			2046-2065			2081-2100		
	min	mean	max	min	mean	max	min	mean	max	min	mean	max
rcp2.6	0.60	0.73	0.81	0.79	0.84	0.89	0.80	0.85	0.89	0.77	0.81	0.86
rcp4.5	0.73	0.84	1.03	0.95	1.02	1.11	1.29	1.36	1.46	1.44	1.53	1.60
rcp6.0	0.64	0.73	0.84	0.78	0.90	1.04	1.16	1.28	1.41	1.73	1.91	2.03
rcp8.5	0.83	0.99	1.22	1.15	1.34	1.53	1.91	2.09	2.24	3.13	3.27	3.42
Range of mean	0.73 – 0.99			0.84 – 1.34			0.85 – 2.09			0.81 – 3.27		

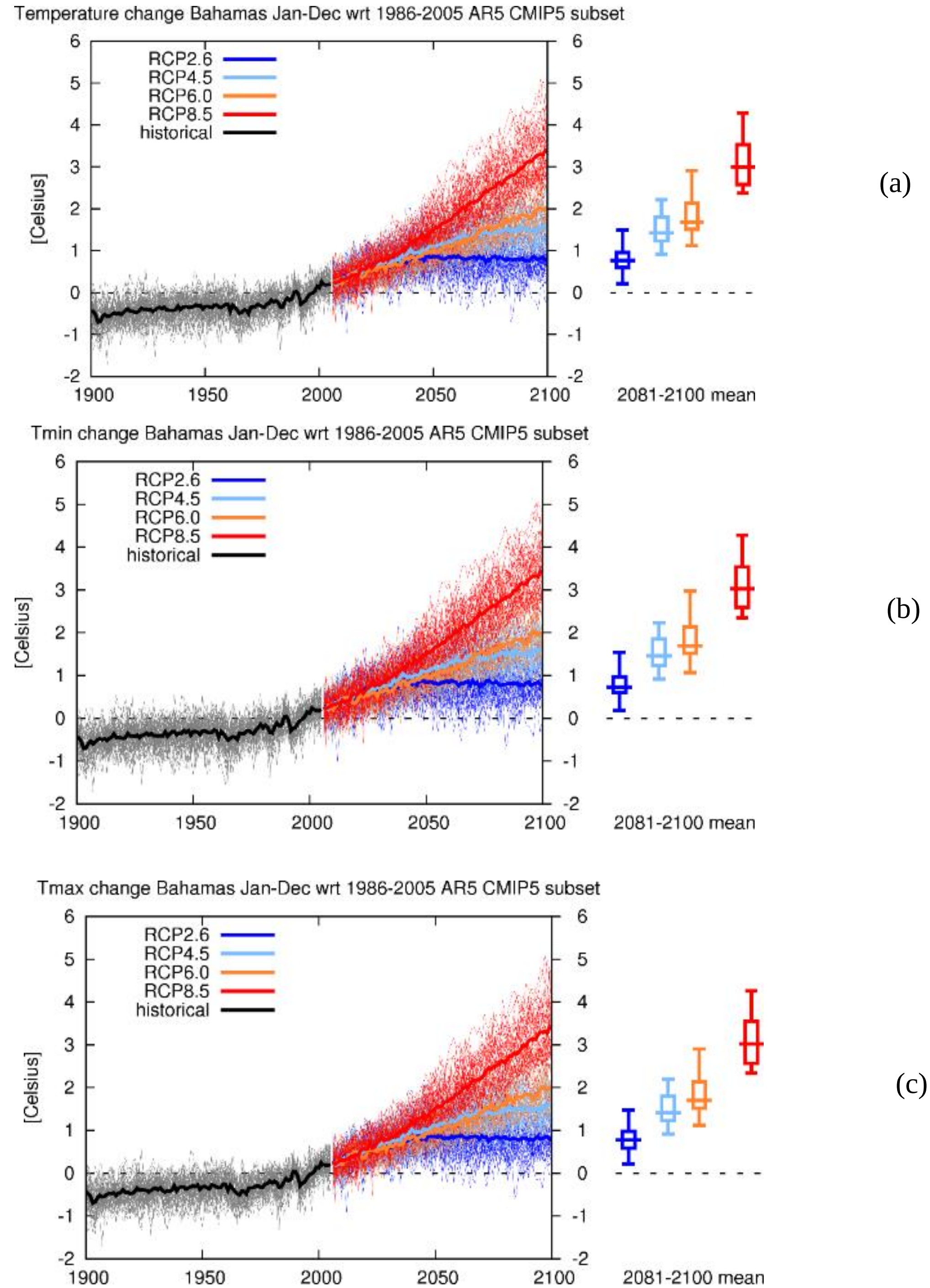

Figure 11: (a) Mean annual temperature change (°C) (b) Mean annual minimum temperature change (°C) (c) Mean annual maximum temperature change (°C) for The Bahamas with respect to 1986-2005 AR5 CMIP5 subset. On the left, for each scenario one line per model is shown plus the multi-model mean, on the right percentiles of the whole dataset: the box extends from 25% to 75%, the whiskers from 5% to 95% and the horizontal line denotes the median (50%). Data Source: AR5 CMIP5 subset, KNMI Climate Change Atlas.

4.4.2 RCM Projections

Tables 7-9, show changes in minimum, mean, and maximum temperatures for the RCM grid boxes covering Great Exuma (3 grid boxes), Eleuthera (7 grid boxes), and Great Abaco (10 grid boxes). Seasonal projections show a general warming across all grid boxes. The mean annual projections indicate that all three islands will experience consistent and sustained warming towards the mid-century.

Table 7: Summary of annual increases in mean, minimum, and maximum temperatures over the grid boxes defined for particular regions of The Bahamas

Region	**2020's (2016-2035)**			**2030's (2026-2045)**			**2050's (2046-2065)**		
	Tmin	Tmean	Tmax	Tmin	Tmean	Tmax	Tmin	Tmean	Tmax
Great Exuma	1.01-1.36	1.01-1.26	1.00-1.30	1.22-1.78	1.22-1.69	1.24-1.76	1.81-3.95	1.81-2.14	-0.04-2.13
Eleuthera	1.08-1.40	1.12-1.27	1.04-1.29	1.17-1.88	1.18-1.74	1.18-1.77	1.92-2.79	1.37-3.21	1.01-4.00
Great Abaco	1.14-1.37	1.04-1.24	1.06-1.36	1.13-1.88	1.14-1.73	1.13-1.87	1.01-2.66	1.40-2.88	1.08-2.68

Table 8-10: Great Exuma - projected absolute change in mean temperature (°C) for the 2020's, 2030's, and 2050's relative to the 1960-1990 baseline. Data presented for minimum, maximum and mean value of a five member ensemble. Values are for 25 km grid boxes shown in Figure 1. Tables arranged by island.

Great Exuma
Table 8: Change in Minimum Temperature (◦C)

GRID BOX	**2020's**			**2030's**			**2050's**		
	MIN	**MEAN**	**MAX**	**MIN**	**MEAN**	**MAX**	**MIN**	**MEAN**	**MAX**
1	1.01	1.09	1.18	1.22	1.40	1.58	1.81	2.15	2.41
2	1.01	1.13	1.31	1.26	1.44	1.73	1.81	2.74	3.59
3	1.01	1.15	1.36	1.28	1.46	1.78	1.81	2.92	3.95

Great Exuma Table 9: Change in Mean Temperature (◦C)									
GRID BOX	**2020's**			**2030's**			**2050's**		
	MIN	**MEAN**	**MAX**	**MIN**	**MEAN**	**MAX**	**MIN**	**MEAN**	**MAX**
1	1.02	1.08	1.13	1..22	1.39	1.53	1.82	1.94	2.09
2	1.01	1.10	1.22	1.24	1.42	1.65	1.81	2.01	2.09
3	1.01	1.11	1.26	1.25	1.43	1.69	1.81	2.04	2.14

Great Exuma Table 10: Change in Maximum Temperature (◦C)									
GRID BOX	**2020's**			**2030's**			**2050's**		
	MIN	**MEAN**	**MAX**	**MIN**	**MEAN**	**MAX**	**MIN**	**MEAN**	**MAX**
1	1.02	1.10	1.17	1.24	1.42	1.60	1.35	1.71	2.13
2	1.01	1.11	1.26	1.24	1.44	1.73	0.24	1.13	2.10
3	1.00	1.11	1.30	1.24	1.45	1.76	-0.04	0.98	2.10

Table 11-13: Eleuthera - projected absolute change in mean temperature (^{o}C) for the 2020's, 2030's, and 2050's relative to the 1961-1990 baseline. Data presented for minimum, maximum and mean value of a five member ensemble. Values are for 25 km grid boxes shown in Figure 1. Tables arranged by regions.

Eleuthera Table 11: Change in Minimum Temperature (◦C)									
GRID BOX	**2020's**			**2030's**			**2050's**		
	MIN	**MEAN**	**MAX**	**MIN**	**MEAN**	**MAX**	**MIN**	**MEAN**	**MAX**
4	1.20	1.26	1.37	1.24	1.53	1.80	2.13	2.27	2.40
5	1.25	1.30	1.41	1.27	1.58	1.86	2.26	2.33	2.44
6	1.18	1.25	1.34	1.25	1.53	1.79	2.07	2.28	2.50
7	1.08	1.15	1.23	1.17	1.41	1.66	2.01	2.08	2.22
8	1.25	1.32	1.40	1.27	1.58	1.88	1.92	2.37	2.74
9	1.25	1.30	1.38	1.26	1.57	1.85	1.61	2.23	2.75
10	1.27	1.31	1.36	1.24	1.57	1.84	1.32	2.10	2.79

Eleuthera Table 12: Change in Mean Temperature (◦C)									
GRID BOX	**2020's**			**2030's**			**2050's**		
	MIN	**MEAN**	**MAX**	**MIN**	**MEAN**	**MAX**	**MIN**	**MEAN**	**MAX**
4	1.12	1.17	1.25	1.23	1.46	1.68	2.04	2.13	2.25
5	1.16	1.21	1.28	1.26	1.49	1.72	2.03	2.23	2.47
6	1.15	1.18	1.23	1.24	1.46	1.69	1.62	2.28	2.73
7	1.05	1.11	1.17	1.18	1.38	1.58	1.79	2.09	2.34
8	1.18	1.22	1.27	1.26	1.49	1.74	1.41	2.44	3.11
9	1.18	1.21	1.26	1.25	1.48	1.73	1.39	2.44	3.16
10	1.18	1.21	1.24	1.23	1.48	1.71	1.37	2.47	3.21

Eleuthera Table 13: Change in Maximum Temperature (◦C)									
GRID BOX	**2020's**			**2030's**			**2050's**		
	MIN	**MEAN**	**MAX**	**MIN**	**MEAN**	**MAX**	**MIN**	**MEAN**	**MAX**
4	1.07	1.15	1.26	1.24	1.44	1.70	1.88	2.05	2.23
5	1.10	1.18	1.29	1.28	1.48	1.76	1.87	2.22	2.56
6	1.12	1.19	1.26	1.29	1.47	1.75	1.27	2.42	3.21
7	1.04	1.11	1.18	1.22	1.40	1.64	1.66	2.18	2.53
8	1.14	1.21	1.29	1.23	1.49	1.81	1.01	2.69	3.86
9	1.13	1.20	1.28	1.18	1.48	1.79	1.34	2.85	3.90
10	1.11	1.19	1.26	1.19	1.48	1.77	1.68	3.10	4.00

Table 14-16: Great Abaco - projected absolute change in mean temperature (^{o}C) for the 2020's, 2030's, and 2050's relative to the 1961-1990 baseline. Data presented for minimum, maximum and mean value of a five member ensemble. Values are for 25 km grid boxes shown in Figure 1. Tables arranged by regions.

Great Abaco Table 14: Change in Minimum Temperature (◦C)									
GRID BOX	**2020's**			**2030's**			**2050's**		
	MIN	**MEAN**	**MAX**	**MIN**	**MEAN**	**MAX**	**MIN**	**MEAN**	**MAX**
11	1.14	1.19	1.29	1.19	1.46	1.77	2.12	2.22	2.40
12	1.14	1.24	1.37	1.25	1.51	1.88	2.26	2.66	3.01
13	1.21	1.26	1.36	1.24	1.53	1.86	2.17	2.39	2.62
14	1.18	1.26	1.37	1.25	1.52	1.87	2.40	2.50	2.60
15	1.18	1.25	1.34	1.23	1.51	1.83	2.04	2.31	2.58
16	1.21	1.24	1.28	1.19	1.49	1.74	1.08	1.87	2.64
17	1.21	1.26	1.33	1.21	1.51	1.80	1.41	2.06	2.68

18	1.20	1.23	1.28	1.17	1.48	1.73	1.01	1.81	2.61
19	1.15	1.18	1.24	1.14	1.42	1.67	1.24	1.79	2.42
20	1.06	1.14	1.25	1.13	1.38	1.68	1.93	2.07	2.17

Great Abaco Table 15: Change in Mean Temperature (◦C)									
GRID BOX	**2020's**			**2030's**			**2050's**		
	MIN	**MEAN**	**MAX**	**MIN**	**MEAN**	**MAX**	**MIN**	**MEAN**	**MAX**
11	1.07	1.14	1.20	1.19	1.41	1.66	1.76	2.22	2.60
12	1.08	1.18	1.26	1.24	1.44	1.73	1.83	2.28	2.61
13	1.10	1.19	1.26	1.23	1.45	1.73	1.58	2.36	2.91
14	1.09	1.19	1.26	1.24	1.45	1.72	1.65	2.32	2.77
15	1.10	1.18	1.24	1.22	1.44	1.70	1.57	2.32	2.85
16	1.12	1.17	1.21	1.19	1.43	1.64	1.38	2.29	2.92
17	1.12	1.19	1.22	1.21	1.44	1.68	1.40	2.34	2.99
18	1.12	1.17	1.19	1.18	1.41	1.63	1.43	2.28	2.88
19	1.09	1.14	1.16	1.15	1.38	1.60	1.64	2.18	2.61
20	1.04	1.11	1.17	1.14	1.36	1.61	1.98	2.10	2.29

Great Abaco Table 16: Change in Maximum Temperature (◦C)									
GRID BOX	**2020's**			**2030's**			**2050's**		
	MIN	**MEAN**	**MAX**	**MIN**	**MEAN**	**MAX**	**MIN**	**MEAN**	**MAX**
11	1.14	1.19	1.29	1.19	1.46	1.77	2.12	2.22	2.40
12	1.14	1.24	1.37	1.25	1.51	1.88	2.26	2.66	3.01
13	1.21	1.26	1.36	1.24	1.53	1.86	2.17	2.39	2.62
14	1.18	1.26	1.37	1.25	1.52	1.87	2.40	2.50	2.60
15	1.18	1.25	1.34	1.23	1.51	1.83	2.04	2.31	2.58
16	1.21	1.24	1.28	1.19	1.49	1.74	1.08	1.87	2.64
17	1.21	1.26	1.33	1.21	1.51	1.80	1.41	2.06	2.68
18	1.20	1.23	1.28	1.17	1.48	1.73	1.01	1.81	2.61
19	1.15	1.18	1.24	1.14	1.42	1.67	1.24	1.79	2.42
20	1.06	1.14	1.25	1.13	1.38	1.68	1.93	2.07	2.17

4.4.3 Extremes Projections

Projected trends in future annual numbers of warm and cool nights indicate a sharp increase in the number of warm nights (+0.69 yr^{-1}) and a gradual decline in the number of cool nights (-0.13 yr^{-1}) beginning around 2020 (Figure 12). The general trends in the temperature extremes over Nassau are consistent with those observed in Stephenson et al. (2014). Table 17 shows the trends in warm and cool nights across the future time slices (2020's, 2030's, 2050's, and end-of-century.

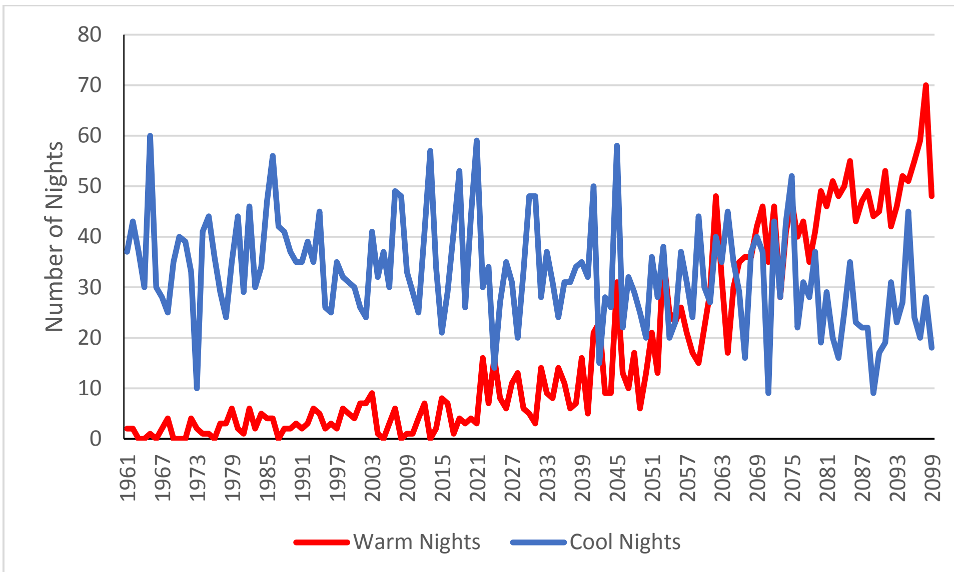

Figure 12: Projections under the A2 scenario for the annual number of warm nights and cool nights for Freeport, Bahamas.

Table 17: Trends, projected under the A2 scenario, in the number of warm nights and cool nights for the 2020's, 2030's, 2050's, and end-of-century (2081-2100).

Time Slices	Warm Nights (yr^{-1})	Cool Nights (yr^{-1})
2020-2029	+0.32	-2.13
2030-2039	+0.60	-1.36
2050-2059	-0.01	+0.89
2081-2100	+0.50	+0.15
2020-2100	+0.69	-0.13

5 Rainfall

5.1 Climatology and Historical Trends

The rainfall climatology for the Bahamas shows two prominent peaks i.e. a bimodal pattern that is characteristic of the Caribbean region (Figure 13). The most prominent peak occurs in June with an average rainfall value of 7.8 mm per day. This major peak is followed by a sharp decline in rainfall during the mid-summer drought (MSD) in July (Magaña et al. 1999, Taylor et al. 2002). The second peak occurs in August and steadily declines until onset of the dry December-February (DJF) season. Figure 14 shows seasonal averages of rainfall (mm day^{-1}). It is to be noted that most of the rainfall received occurs between June and November.

Figure 13 also indicates differences between the climatologies for 1961-1990 versus 1991-2011. In more recent times there has been a slight increase in rainfall in the dry season (February-March) as well as in September and November, and a decrease in rainfall in July and October. Figure 14 similarly shows the general trend in rainfall for the two periods but across seasons. The late rainy season (July onwards) has seen an increase in rainfall in the more recent 20 year period resulting in a mean annual increase. Rainfall averages across JJA, ASO, and SON seasons all indicate an increase during the 1991-2014 period over the 1961-1990 period. This is also consistent with observed increases in tropical cyclone events beginning in the early 1990's and continuing into the 2000's.

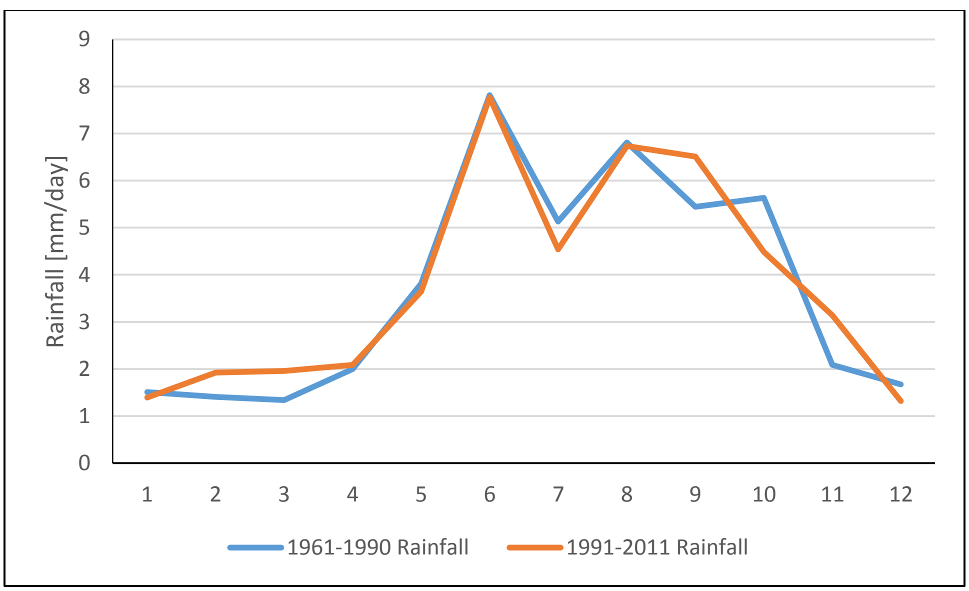

Figure 13: Climatology for rainfall for the periods 1961-1990 and 1991-2011. Rainfall is measured in mm per day. Data Source: RClimDex.

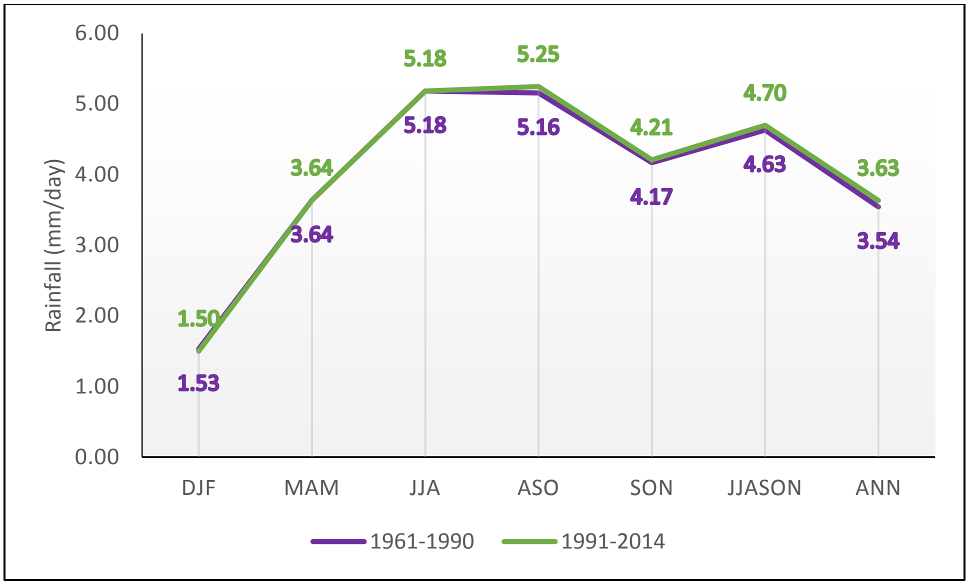

Figure 14: Seasonal averages for rainfall in mm per day for The Bahamas for the period 1961-1990 (purple) and 1991-2014 (green). Data Source: CRU TS3.23.

Figure 15 shows the 1901-2014 trend in mean rainfall (given in mm per month) over the Bahamas from the CRU data. It is a positive trend reflecting an increase per year of 0.092 mm $month^{-1}$. The data also suggests positive trends across the island group ranging from +0.12 (Grand Bahama) to +0.20 (Nassau International, Nassau) (Table 18). There is, however, considerable interannual and decadal variability (see also section 5.3). That is, notwithstanding the overall trend, (for example) the period since 2000 to present was drier than the fifteen year prior period from 1985 to 2000 (Figure 15).

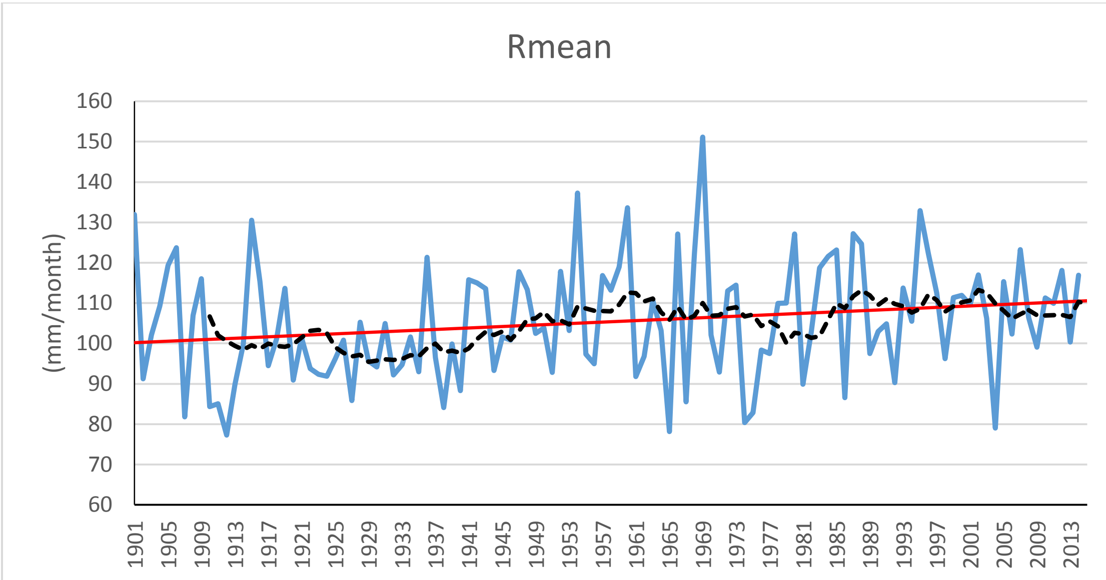

Figure 15: The annual mean rainfall for the Bahamas for 1901-2014. The linear trend is indicated with a red solid line, while the black broken line indicates the 10-year moving average. Data Source: CRU TS3.23.

Table 18: Trends in mean rainfall (mm $month^{-1}$) each year for locations across the Bahamas. Data Source: CRU TS3.23.

Location	Trend in Rmean (mm $month^{-1}$ $year^{-1}$)
Eleuthera	+0.17
Georgetown, Great Exuma	+0.13
Grand Bahama	+0.12
Marsh Harbour, Great Abaco	+0.13
Nassau International, Nassau	+0.20
The Bahamas (overall)	+0.09

5.2 Rainfall Extremes

5.2.1 Caribbean

Stephenson et al. (2014) indicate that Caribbean rainfall extremes show small (though statistically insignificant) increases for the period 1961-2010 for stations north of Cuba. Figure 16 shows that total precipitation (PRCPTOT) has a general positive trend for the northern regions of the Bahamas over the 1961-2010 period. This is in agreement with Figure 15. The simple daily intensity index (SDII) also shows a small increase over the Bahamas. However for the latter period 1986-2010, the northern section of the Bahamas shows a decline in the PRCPTOT index. There is for the same period an increase in the SDII value. Consecutive dry days (CDD) for the Bahamas, and the Caribbean at large, show a consistent drying for both 1961-2010 and 1986-2010.

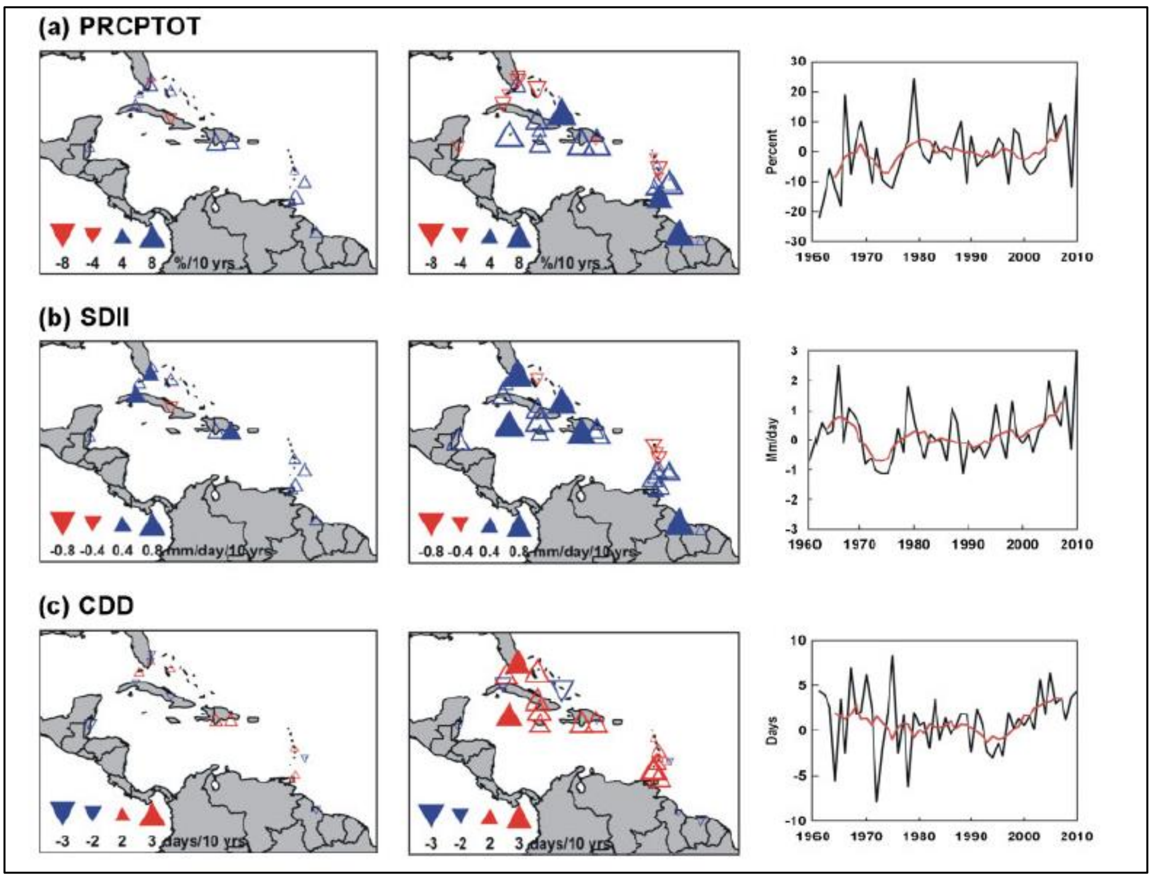

Figure 16: Same as Figure 9 but for the trends in (a) total precipitation (PRCPTOT), (b) simple daily intensity index (SDII) and (c) consecutive wet days (CDD). Blue colour indicates trends toward wetter conditions and red indicates drying trends in (a) and (b). Red colour in (c) indicates trends toward a longer drying spell.

5.2.2 Nassau, Bahamas

Table 19 lists historical trends in rainfall extremes over Nassau for the period 1981-2001 as calculated from available station data. There is a general increasing trend for most extremes indices but a decline in the number of days rainfall was above 10mm and 20mm thresholds.

Table 19: Historical trends in extreme rainfall indices across 1981-2001. Data shown for total precipitation (PRCPTOT) in mm yr^{-1}; consecutive dry days (CDD) in days yr^{-1}; annual count of days above 10 mm (R10mm) [1], 20 mm (R20mm), 50 m (R50mm) in days yr; very wet days (R95p) in mm yr^{-1}; maximum 1-day precipitation (RX1) in mm yr^{-1}; maximum 5-day precipitation (RX5) in mm yr^{-1}.

Index	Trend across 1981-2001
PRCPTOT	+19.01
CDD	+0.19
R10mm	-0.04
R20	-0.07
R50	+0.19
R95p	+17.90
RX1	+3.38
RX5	+6.20

5.3 Variability

The variance in rainfall anomalies over the Caribbean indicates that linear trends do not contribute significantly to variations in rainfall (only 1%). The majority of Caribbean rainfall variability is accounted for by inter-annual variability (88%), and decadal variability (8%) (Figure 17). It is the dominance of the inter-annual (i.e. year to year swings in extremes in the total rainfall) that results in the small linear trends. Swings in the rainfall anomalies over the Bahamas mirror this and are driven predominantly by inter-annual variability (82%) and decadal variability (13%) (Figure 17).

(A)

The Caribbean

Trend	1%
Decadal	8%
Inter-annual	88%

(B)

The Bahamas

Trend	0%
Decadal	13%
Inter-annual	82%

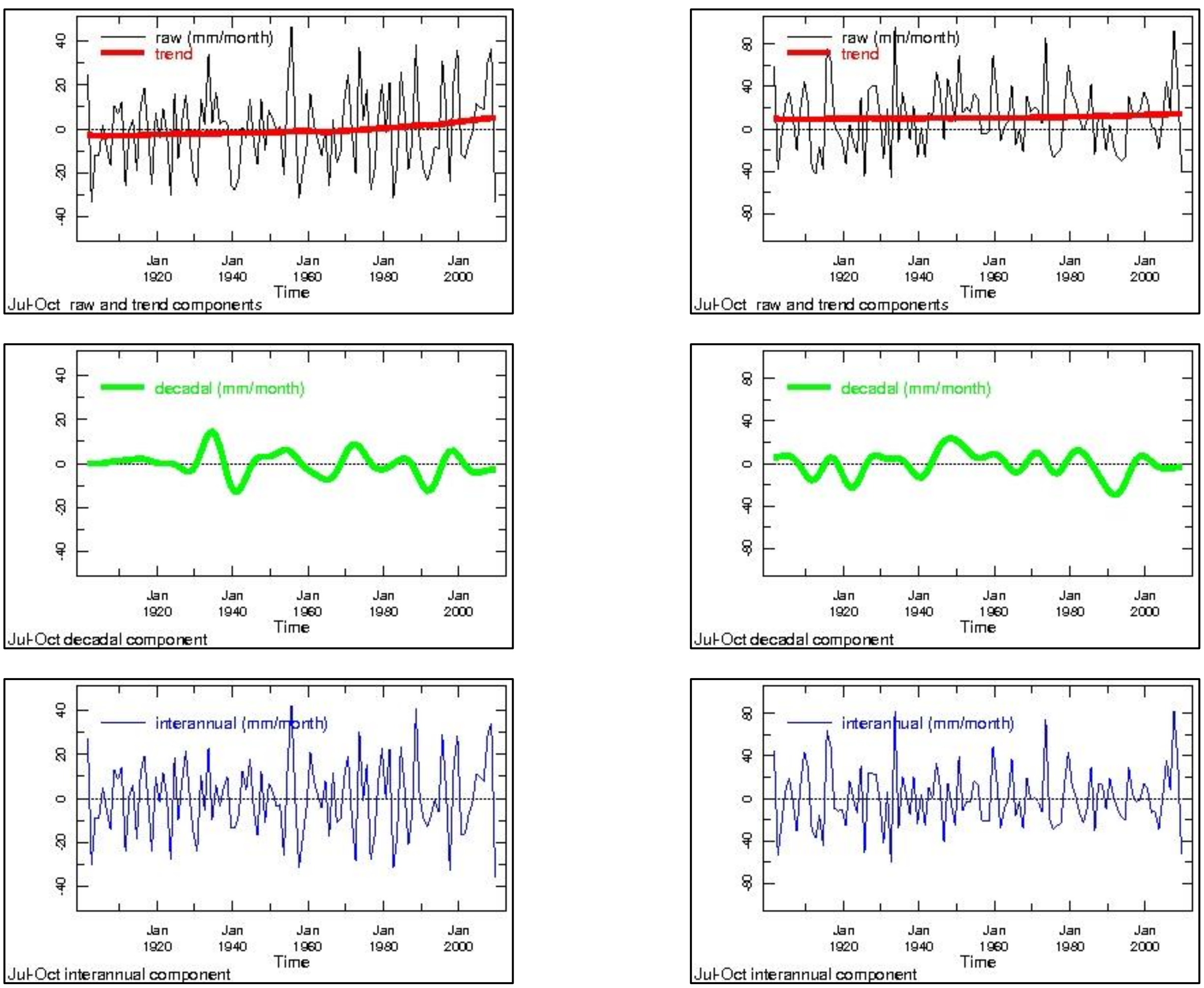

Figure 17: Average July-October rainfall anomalies over (A) the Caribbean (left panel) and (B) the Bahamas (right panel) from the late 1800s with trend line imposed. For each panel, the percentage of variance explained by trend line, decadal variations (> 10 years), and inter-annual (year-to-year) variations. Data source: CRU TS3.10. Acknowledgements: IRI Map Room.

5.4 Projections

5.4.1 GCM Projections

Tables 20-22 show the projected percentages changes in annual precipitation for the four RCP scenarios as projected by an ensemble of GCMs. Under the more moderate future scenarios (RCP2.6 and RCP4.5), the Bahamas get slightly wetter (1-2%) in the mean through to the end of the century. Under the more severe emission scenarios, however, the Bahamas progressively dries (1.5 to 5% drier by the end of century). Up to the mid-century, variability again seems to dominate. It is a drying in the wet season (August to November) that seems to contribute to the end-of-century drying under the more sever scenarios. Dry season rainfall seems to slightly increase toward the end of the century under all scenarios. Figure 18 shows a graphical representation of projections for the wet season (August-November) and the dry season (December-March) with respect to 1986-2005.

Table 20: Mean percentage change in rainfall for The Bahamas with respect to 1986-2005. Change shown for four RCP scenarios. Data Source: AR5 CMIP5 subset, KNMI Climate Change Atlas.

	Annual Precipitation (% change)											
Centered on	**2020's**			**2030's**			**2050's**			**EOC**		
Averaged over	**2020-2029**			**2030-2039**			**2050-2059**			**2081-2100**		
	min	**mean**	**max**	**min**	**mean**	**max**	**min**	**mean**	**max**	**min**	**mean**	**max**
rcp2.6	-12.36	2.74	11.17	-2.03	3.90	10.64	-3.08	8.87	21.13	-9.17	7.16	20.02
rcp4.5	-19.85	4.75	11.17	-11.24	1.86	13.50	-18.92	-4.40	14.69	-10.72	3.16	16.46
rcp6.0	-18.96	-3.93	12.62	-7.41	-0.15	8.23	-7.44	1.92	10.91	-17.15	-5.33	8.22
rcp8.5	-5.89	2.89	9.03	-7.88	-1.05	13.10	-12.33	-1.79	7.77	-31.09	-19.68	-4.49
Range of mean	**-3.93 – 4.75**			**-1.05 – 3.90**			**-4.40 – 8.87**			**-19.68 – 7.16**		

Table 21: Mean percentage change in summer rainfall (August–November) for The Bahamas with respect to 196-2005. Change shown for four RCP scenarios. Data Source: AR5 CMIP5 subset, KNMI Climate Change Atlas.

	Wet season Precipitation (% change)											
	2020's			**2030's**			**2050's**			**EOC**		
Averaged over	**2020-2029**			**2030-2039**			**2050-2059**			**2081-2100**		
	min	**mean**	**max**	**min**	**mean**	**max**	**min**	**mean**	**max**	**min**	**mean**	**max**
rcp2.6	-14.40	7.99	29.37	-18.30	2.89	26.49	-6.84	13.01	36.02	-21.98	7.16	30.37
rcp4.5	-28.95	12.55	32.67	-13.60	4.16	20.53	-23.41	-4.09	14.21	-11.74	11.23	34.90
rcp6.0	-21.68	-3.38	10.31	-17.06	1.58	20.53	-14.63	7.01	33.21	-43.21	-0.63	30.53
rcp8.5	-10.87	6.49	16.71	-19.37	6.16	26.30	-27.21	4.81	16.46	-38.21	-12.43	21.74
Range of mean	**-3.38 – 12.55**			**1.58 – 6.16**			**-4.09 – 13.01**			**-12.43 – 11.23**		

Table 22: Mean percentage change in dry season rainfall (December-March) for The Bahamas with respect to 196-2005. Change shown for four RCP scenarios. Data Source: AR5 CMIP5 subset, KNMI Climate Change Atlas.

	Dry season Precipitation (% change)											
	2020's			**2030's**			**2050's**			**EOC**		
Averaged over	**2020-2029**			**2030-2039**			**2050-2059**			**2081-2100**		
	min	**mean**	**max**	**min**	**mean**	**max**	**min**	**mean**	**max**	**min**	**mean**	**max**
rcp2.6	-22.65	4.90	18.19	-1.94	18.68	29.87	4.80	14.17	32.51	-4.86	10.55	28.26
rcp4.5	-9.19	5.73	24.80	-4.18	5.18	16.79	0.20	13.65	31.63	-4.49	11.84	30.72
rcp6.0	-9.82	1.24	13.86	-11.13	6.26	23.56	-18.38	-2.23	26.37	-9.61	5.87	19.58
rcp8.5	-19.04	5.78	29.67	-12.05	4.58	21.99	-9.11	9.09	27.07	-14.84	2.94	29.30
Range of mean	**1.24 – 5.78**			**4.58 – 18.68**			**-2.23 – 14.17**			**2.94 – 11.84**		

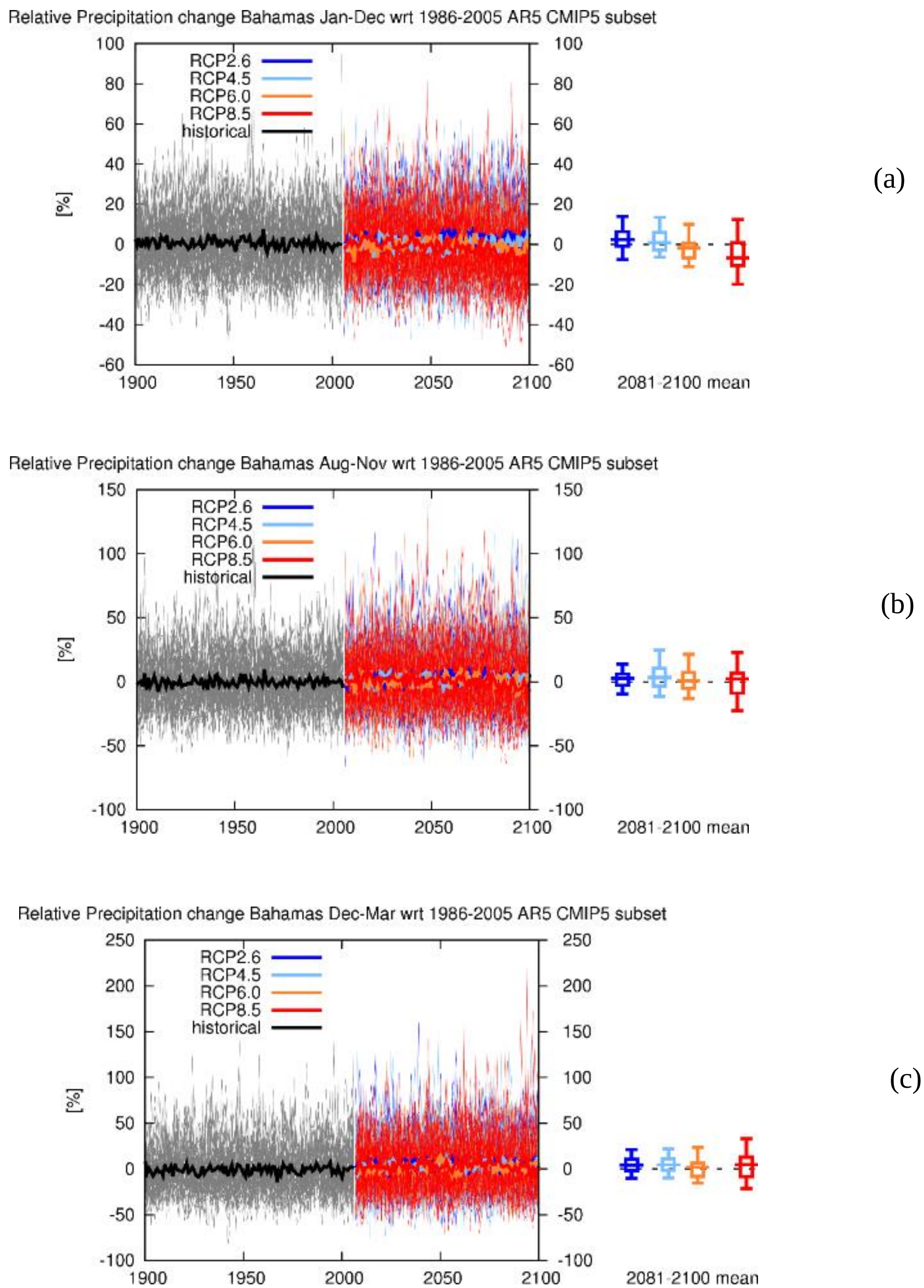

Figure 18: (a) Relative annual precipitation change (oC) (b) Relative August-November precipitation change (oC) (c) Relative December-March precipitation change (oC) for The Bahamas with respect to 1986-2005 AR5 CMIP5 subset. On the left, for each scenario one line per model is shown plus the multi-model mean, on the right percentiles of the whole dataset: the box extends from 25% to 75%, the whiskers from 5% to 95% and the horizontal line denotes the median (50%). Data Source: AR5 CMIP5 subset, KNMI Climate Change Atlas.

5.4.2 RCM Projections

Table 23 summarizes the range of annual percentage changes in precipitation for the islands of Great Exuma, Eleuthera, and Great Abaco, as projected by a subset of GCMs from phase 5 of the Coupled Model Intercomparison Project (CMIP5) spearheaded by the IPCC. The projections suggest increased variability in rainfall toward at least the mid-century. There is also the suggestion that the Bahamas may be slightly wetter approaching mid-century, which is in contrast to the rest of the Caribbean. This has also been noted in previous projection studies for the region (e.g. Campbell et al. 2011). Tables 24-26 below provides the minimum, mean, and maximum annual percentage change in precipitation for each of the three islands in the 2020's, 2030's, and 2050's. Projected percentage changes in precipitation are averaged for 25-km grid boxes across Great Exuma, Eleuthera, and Great Abaco. Please refer to Figure 1 in Section 3 highlighting the distribution of grid boxes across the islands of interest.

Table 23: Summary of annual percentage changes in precipitation over the grid boxes defined for particular regions of The Bahamas.

Region	2020's (2016-2035)	2030's (2026-2045)	2050's (2046-2065)
Great Exuma	-8.23 – 25.96	-10.21 – 21.10	-13.63 – 58.46
Eleuthera	-9.82 – 20.61	-4.97 – 11.82	-17.87 – 43.14
The Abacos	-4.27 – 20.29	-4.34 – 17.47	-11.87 – 26.48

Table 24-26: Projected percentage change in annual rainfall for the 2020's, 2030's, and 2050's relative to the 1986-2005 baseline. Data presented for minimum, maximum, and mean value of a five-member ensemble. Values for 25-km grid boxes shown in Figure 1. Tables are arranged by region.

Great Exuma
Table 24: Percentage change in Precipitation (%)

GRID BOX	2020's			2030's			2050's		
	MIN	MEAN	MAX	MIN	MEAN	MAX	MIN	MEAN	MAX
1	-6.16	5.27	23.72	-6.05	8.02	17.48	-13.63	0.74	12.81
2	-5.96	7.48	25.96	-8.27	7.82	20.58	3.16	11.27	30.89
3	-8.23	6.80	25.27	-10.21	6.18	21.10	2.98	23.17	58.46

Eleuthera Table 25: Percentage change in Precipitation (%)									
GRID BOX	**2020's**			**2030's**			**2050's**		
	MIN	**MEAN**	**MAX**	**MIN**	**MEAN**	**MAX**	**MIN**	**MEAN**	**MAX**
4	-4.27	6.37	20.29	-4.34	1.43	10.35	-11.27	3.79	20.68
5	-3.67	3.44	16.60	-5.63	-0.32	10.22	-11.87	0.98	15.79
6	-1.83	3.91	14.49	-4.18	1.70	13.57	-6.99	4.40	14.03
7	0.95	7.72	16.76	-4.08	4.61	17.47	-8.37	8.12	26.48
8	-2.26	1.62	10.08	-4.25	0.78	13.53	-9.26	0.25	9.84
9	-0.79	2.95	9.94	-6.29	1.46	17.35	-10.99	-2.09	9.22
10	1.26	3.89	8.40	-4.37	1.35	13.87	-9.20	-3.66	3.21

Great Abaco Table 26: Percentage change in Precipitation (%)									
GRID BOX	**2020's**			**2030's**			**2050's**		
	MIN	**MEAN**	**MAX**	**MIN**	**MEAN**	**MAX**	**MIN**	**MEAN**	**MAX**
11	-0.81	3.36	11.68	-4.29	1.32	11.82	-9.12	2.19	9.72
12	-1.52	3.32	12.40	-3.48	1.04	8.61	-11.08	11.79	34.80
13	-3.10	3.28	12.35	-4.55	1.98	11.08	-8.31	7.65	20.75
14	-2.30	3.33	10.46	-2.32	0.76	5.55	-12.36	13.31	43.14
15	-2.84	3.37	10.11	-1.10	1.59	7.86	-6.79	8.93	25.86
16	-2.94	3.67	7.70	-2.84	0.65	4.02	-12.46	4.44	26.57
17	-4.52	3.07	10.41	-1.79	0.92	4.81	-7.07	2.94	15.15
18	-5.24	1.28	11.60	-4.26	-0.94	4.28	-9.45	0.91	17.05
19	-7.71	1.36	15.50	-4.97	-2.49	1.08	-13.20	-0.34	18.09
20	-9.82	2.34	20.61	-4.19	-2.22	0.13	-17.87	1.94	27.64

5.4.3 Rainfall Extremes

Table 27 below compares the trends in projected rainfall extremes for the Nassau station data under the SRES B2 (low emissions) scenario and A2 (high emissions) scenario. The A2 and B2 scenarios present contrasting pictures in the short term. In the 2020s, under the A2 (B2) scenario the rainfall indices generally suggest wetter (drier) conditions.

Table 27: Trends in projected rainfall extremes under the B2 and A2 scenarios for the 2020's, 2030's, 2050's, and end-of-century. Data shown consecutive dry days (CDD) in days yr^{-1}; annual count of days above 10 mm (R10mm) [1], 20 mm (R20mm), 50 m (R50mm) in days yr; very wet days (R95p) in mm yr^{-1}; maximum 1-day precipitation (RX1) in mm yr^{-1}; maximum 5-day precipitation (RX5) in mm yr^{-1}.

	2020's		2030's		2050's		EOC	
	2020-2029		2030-2039		2050-2059		2081-2100	
	B2	A2	B2	A2	B2	A2	B2	A2
CDD	+0.16	-0.55	-0.35	-0.08	-0.35	-0.01	-0.12	+0.27
R10mm	+0.01	-0.04	+0.86	-0.04	-1.04	-0.65	+0.74	+0.88
R20	-0.21	+0.03	+0.40	+0.30	+0.26	-0.14	+0.26	+0.48
R50	-0.06	+0.02	-0.05	+0.04	0.00	+0.03	-0.01	+0.06
R95p	-11.50	+2.88	+16.25	+14.11	+7.53	-6.76	+9.01	+19.49
RX1	-2.65	+1.47	-1.69	+0.21	-0.23	-0.09	-2.00	+1.28
RX5	-1.43	+1.74	+1.81	-1.07	-0.11	-2.34	-0.19	+2.29

6 Hurricanes

6.1 Historical Trends

6.1.1 Atlantic

Every year, beginning in May and ending in November, the North Atlantic region experiences conditions favorable to tropical cyclone (TC) development: i) a decrease in vertical wind shear, ii) a weakening of easterly trade winds, iii) sea surface temperatures (SSTs) are greater than 26°C (Klotzbach 2007; Goldenberg et al. 2001; Webster et al. 2005). Tropical cyclone activity is also dependent on large-scale atmospheric dynamics, such as the El Niño Southern Oscillation (ENSO) and the Atlantic Multidecadal Oscillation (AMO). When ENSO is in its positive phase (therefore, anomalously warm SSTs are observed in the equatorial Pacific), TC activity in the North Atlantic is suppressed, particularly for the Caribbean (Chu 2004). During its negative phase (known as La Niña), the equatorial Pacific experiences anomalously cooler SSTs and North Atlantic TC activity is enhanced. Studies such as Goldenberg et al. (2005) also indicate that enhanced TC activity is observed in the North Atlantic when the AMO is in its positive phase.

Tropical cyclone activity is measured with a variety of metrics for intensity, frequency, and duration. Storm records for the North Atlantic region can date as far back as the mid-1800's. While recent reanalysis of observational datasets have been able to convey reasonable depictions of North Atlantic TC trends from the early 1900's to present, we limit our analysis of TC records to the instrumental period beginning in the mid 1950's. This period signifies the use of air craft reconnaissance, with an introduction of satellite imagery by the late 1970's, to verify the state of tropical storms.

The total number of storms passing through the North Atlantic region since 1850 is illustrated in Figure 19. The North Atlantic has seen an increase in tropical cyclone activity since 1995 with a distinct increase in the number of intense (category 4 and 5) storms (Webster et al. 2005). In Figure 20, TCs are shown to be most likely to occur within the Caribbean during the height of the season (August-October) before moving poleward along the US eastern coast.

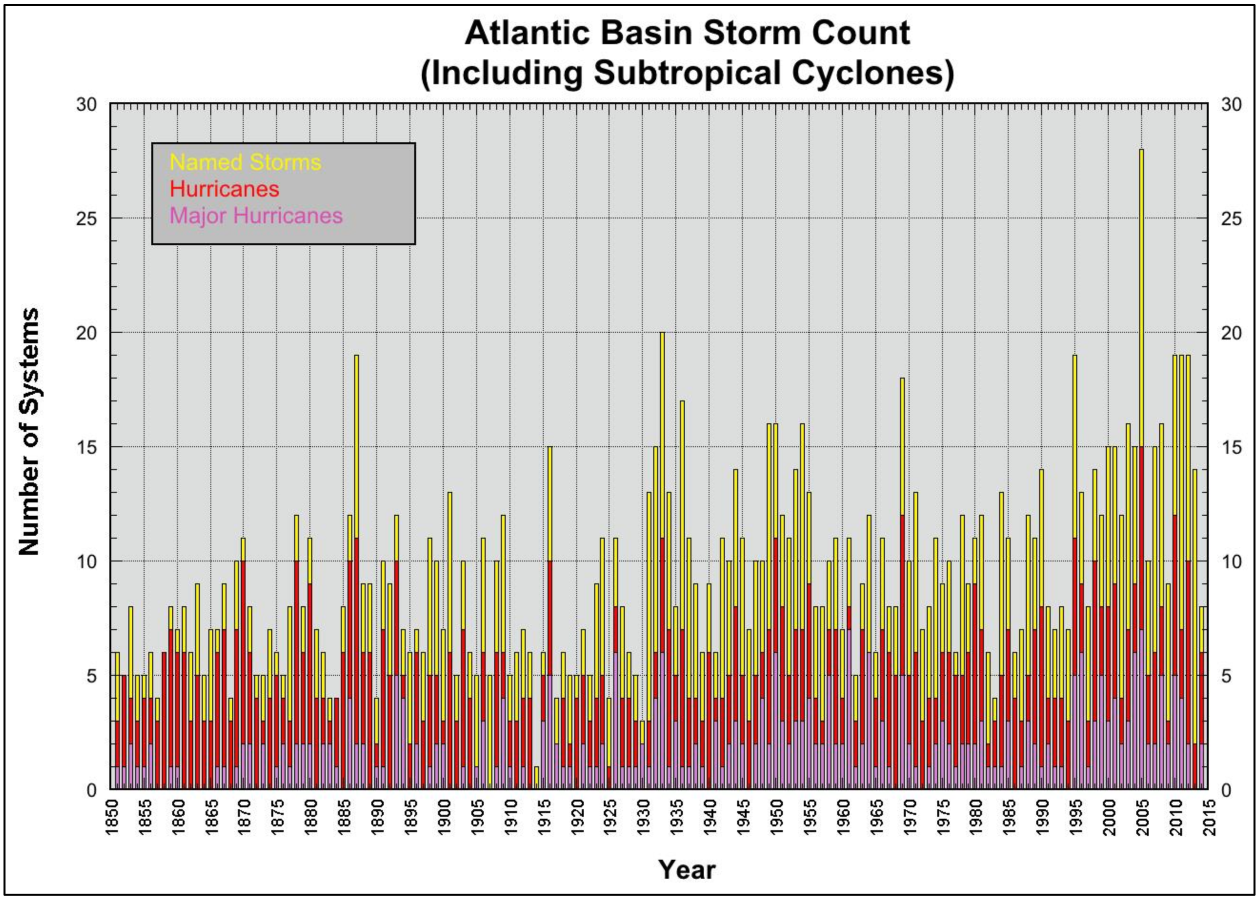

Figure 19: The number of named storms, hurricanes and major hurricanes per year passing through the North Atlantic and Gulf of Mexico from 1850 to present. Source: NOAA.

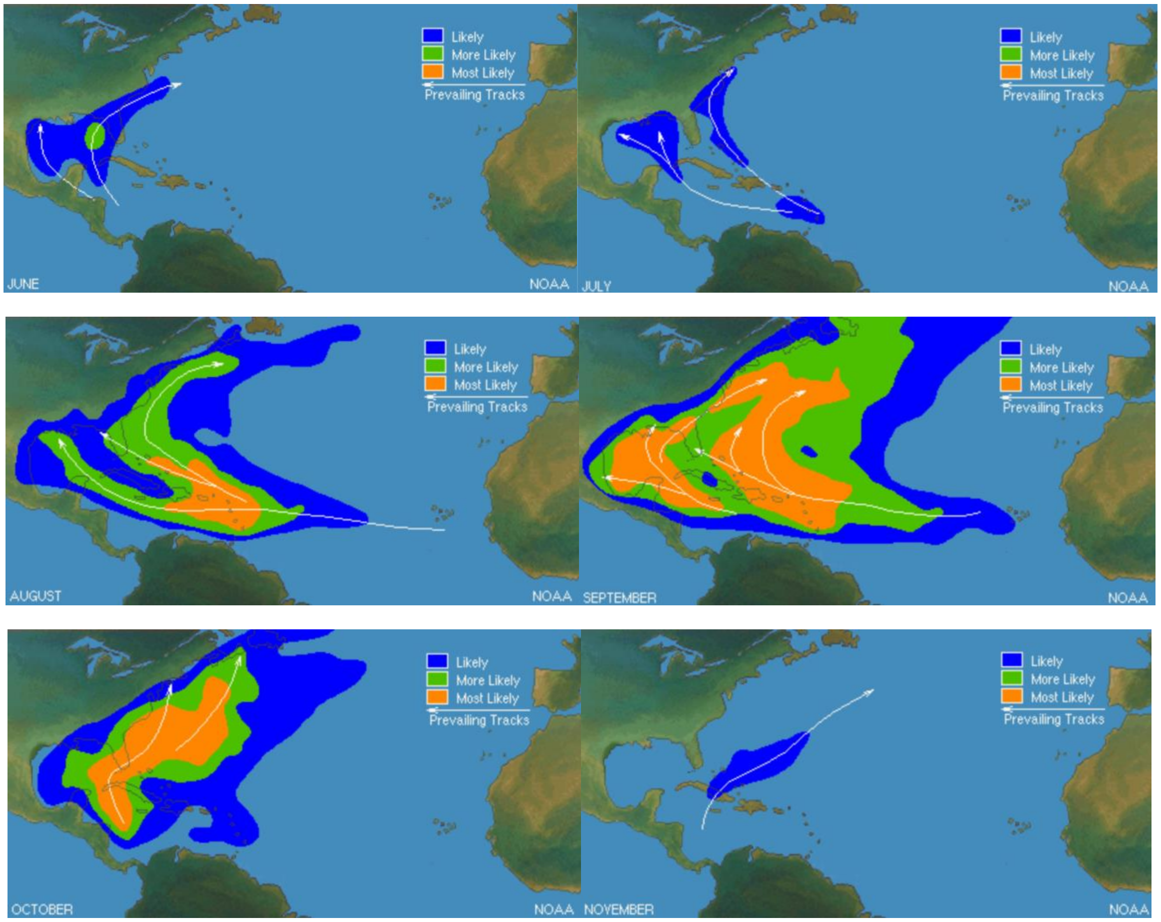

Figure 20: Zones of likely origin and track density of storms by month during the hurricane season from June-November. Source: NOAA.

6.1.2 The Bahamas

The Bahamas islands are located in a track-dense region of the Caribbean, as shown in Figure 20 above. There are a substantial number of tropical cyclones recorded to have passed through and very close by the islands on their way poleward to the subtropical North Atlantic. Figure 21 below shows the progression of tropical cyclones passing within a 100-km radius of Great Exuma, Eleuthera and Abaco from 1950 to 2015. The grid boxes over Eleuthera are the most affected by tropical cyclones, as indicated in Tables 28-30. Eleuthera also has the largest number of land-falling systems (see Tables 31-33).

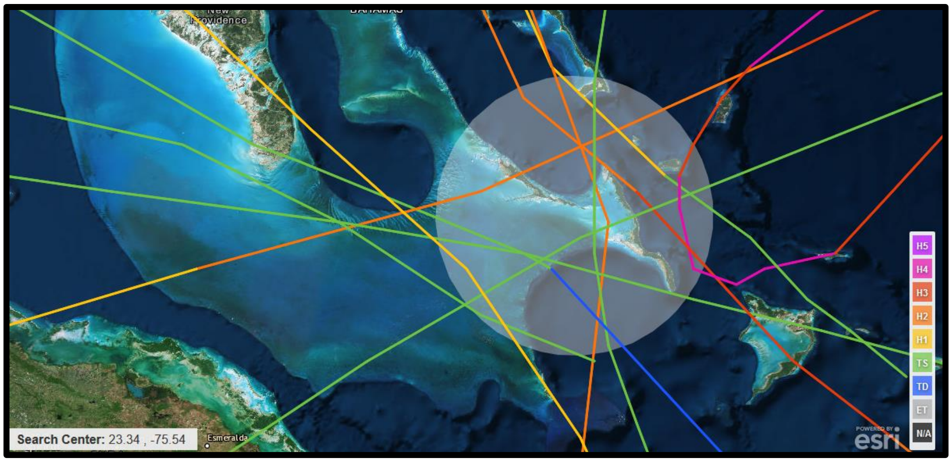

a)

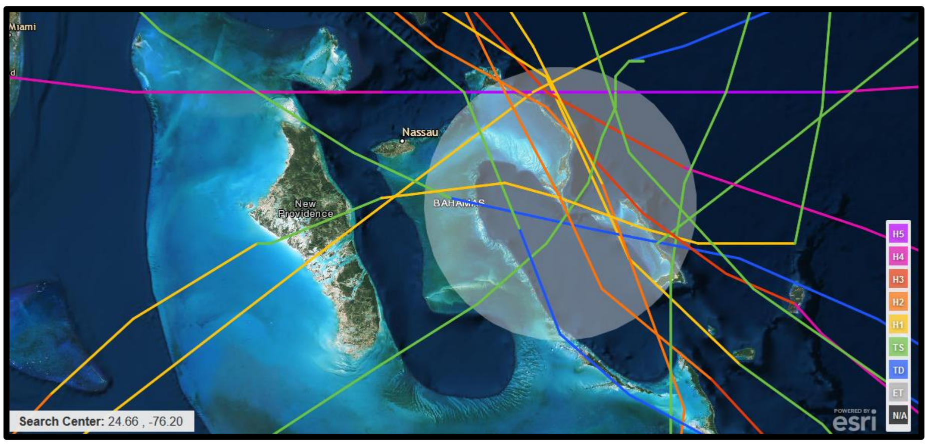

b)

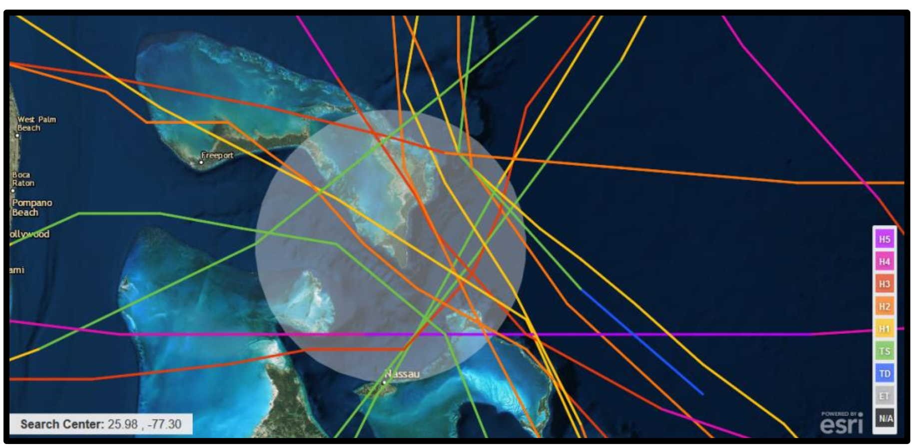

c)

Figure 21: Tropical cyclones of tropical storm strength and greater passing within a 100-km radius of a) Great Exuma, b) Eleuthera, and c) Abaco from 1950 to 2015. Source: NOAA.

Table 28: The number of hurricanes (by category) passing within 100-km radius of Great Exuma (centered on 23.34°N, 75.54°W) from 1950 to 2015. Impact on grid boxes previously defined are shown.

		Grid Box		
		1	2	3
Category	1	2	2	2
	2	3	3	3
	3	1	0	0
	4	0	0	0
	5	0	0	0
		6	5	5
		Number of Hurricanes Impacting Grid Box		

Table 29: The number of hurricanes (by category) passing within 100-km of Eleuthera (centered on 24.66°N, 76.2°W) from 1950 to 2015. Impact on grid boxes previously defined are shown.

		Grid Box						
		4	5	6	7	8	9	10
Category	1	3	3	4	5	4	4	6
	2	2	2	2	2	3	3	2
	3	2	3	4	4	3	3	3
	4	0	0	0	0	0	0	0
	5	1	2	2	2	2	2	2
		8	10	12	13	12	12	13
		Number of Hurricanes Impacting Grid Box						

Table 30: The number of hurricanes (by category) passing within 100-km of Abaco (centered on 25.98°N, 77.3°W) from 1950 to 2015. Impact on grid boxes previously defined are shown.

		Grid Box									
		11	12	13	14	15	16	17	18	19	20
Category	1	1	2	2	3	2	2	2	2	1	2
	2	2	3	2	1	2	1	1	1	0	1
	3	1	1	1	3	2	3	2	2	2	2
	4	0	0	0	0	0	0	0	0	0	0
	5	0	0	0	0	0	0	0	0	0	0
		4	6	5	7	6	6	5	5	3	5
		Number of Hurricanes Impacting Grid Box									

Table 31-33: Named storms by decade that passed within 100-km radius of Great Exuma, Eleuthera, and Great Abaco. The table also indicates the category of storms affecting the island and whether the storm made landfall.

Table 31. Great Exuma (23.34°N, 75.54°W)				
Decades	Year	Name	Highest Category	Landfall
1950-1959	1952	FOX	1	L
1960-1969	1960	DONNA	3	L
1970-1979	1979	DAVID	1	
1990-1999	1995	ERIN	1	
	1996	LILI	2	
2000-2009	2004	FRANCES	3	L
2010-2019	2011	IRENE	2	L
	2012	SANDY	2	
	2015	JOAQUIN	3	L

Table 32. Eleuthera (24.66°N, 76.2°W)				
Decades	Year	Name	Highest Category	Landfall
1950-1959	1952	FOX	1	L
	1954	EDNA	1	
	1956	BETSY	3	
	1958	JANICE	0	L
1960-1969	1965	BETSY	3	
1970-1979	1979	DAVID	1	
1990-1999	1992	ANDREW	5	L
	1995	ERIN	1	
	1996	BERTHA	1	
	1996	LILI	2	
	1999	DENNIS	1	
	1999	FLOYD	3	L
2000-2009	2001	MICHELLE	1	L
	2004	FRANCES	3	L
2010-2019	2011	IRENE	2	L
	2012	SANDY	2	

Table 33. Great Abaco (25.98°N, 77.30°W)				
Decades	Year	Name	Highest Category	Landfall
1950-1959	1956	BETSY	3	
	1958	JANICE	0	L
1960-1969	1965	BETSY	3	
1990-1999	1992	ANDREW	5	L
	1995	ERIN	1	
	1999	DENNIS	1	L
	1999	FLOYD	3	L
2000-2009	2004	FRANCES	2	
	2004	JEANNE	3	L
	2007	NOEL	1	
2010-2019	2011	IRENE	2	L
	2012	SANDY	1	

6.2 Projections

The IPCC Special Report on Extremes (IPCC 2012) offers five summary statements with respect to projections of future hurricane under global warming which are of relevance to the Bahamas and the Caribbean sub-region at large. They are reiterated below as major conclusions and supported with additional information (where available) specific for the Atlantic basin.

Conclusion 1: There is low confidence in projections of changes in tropical cyclone genesis, location, tracks, duration, or areas of impact.

Tropical cyclone genesis and track variability is modulated in most regions by known modes of atmosphere–ocean variability. The details of the relationships vary by region (e.g., El Niño events tend to suppress Atlantic storm genesis and development). The accurate modelling, then, of tropical cyclone activity fundamentally depends on the model’s ability to reproduce these modes of variability i.e. to produce reliable projections of the behaviour of these modes of variability (e.g., ENSO) under global warming, as well as on a good understanding of their physical links with tropical cyclones. At present there is still uncertainty in the model’s ability to project these behaviours.

Conclusion 2: Based on the level of consistency among models, and physical reasoning, it is likely that tropical cyclone related rainfall rates will increase with greenhouse warming.

Observed changes in rainfall associated with tropical cyclones have not been clearly established. However, as water vapor in the tropics increases there is an expectation for increased heavy rainfall associated with tropical cyclones. Models in which tropical cyclone precipitation rates have been examined are highly consistent in projecting increased rainfall within the area near the tropical cyclone center under 21st century warming, with increases of 3 to 37% (Knutson et al., 2010). Typical projected increases are near 20% within 100 km of storm centers (see Figure 22). More recent work premised on RCP 4.5 suggest that rainfall rates increase robustly for the CMIP3 and CMIP5 scenarios (Knutson et al. 2013). For the late-twenty-first century, the increase amounts to +20% to +30% in the model hurricane's inner core, with a smaller increase (~10%) at radii of 200 km or larger.

Conclusion 3: It is likely that the global frequency of tropical cyclones will either decrease or remain essentially unchanged.

Hurricane research done at NOAA's GFDL laboratory using regional models projects that Atlantic hurricane and tropical storms are **substantially reduced in number,** for the average 21st century climate change projected by current models, but will have **higher rainfall rates**, particularly near the storm center. http://www.gfdl.noaa.gov/global-warming-and-hurricaneshttp://www.gfdl.noaa.gov/global-warming-and-hurricanes

Conclusion 4: An increase in mean tropical cyclone maximum wind speed is likely, although increases may not occur in all tropical regions.

Assessments of projections by Knutson et al. (2010) and Bender et al. (2010) and by statistical-dynamical models (for e.g. (Emanuel 2007)) are consistent in that greenhouse warming causes tropical cyclone intensity to shift toward stronger storms by the end of the 21st century as measured by maximum wind speed increases by +2 to +11%. Figure 23 illustrates the increase in the frequency of intense storms in a warmer climate.

Conclusion 5: While it is likely that overall global frequency will either decrease or remain essentially unchanged, it is more likely than not that the frequency of the most intense storms will increase substantially in some ocean basins.

The downscaling experiments of Bender et al. (2010) project a 28% reduction in the overall frequency of Atlantic storms and an 80% increase in the frequency of Saffir-Simpson category 4 and 5 Atlantic hurricanes over the next 80 years using the A1B scenario. Downscaled projections using CMIP5 multi-model scenarios (RCP4.5) as input (Knutson et al. 2013) still show increases in category 4 and 5 storm frequency, but these are only marginally significant for the

early 21st century (+45%) or the late 21st century (+40%) using CMIP5 scenarios. Refer to Figure 24 for a comparison of trends in TC activity across the globe and select ocean basins.

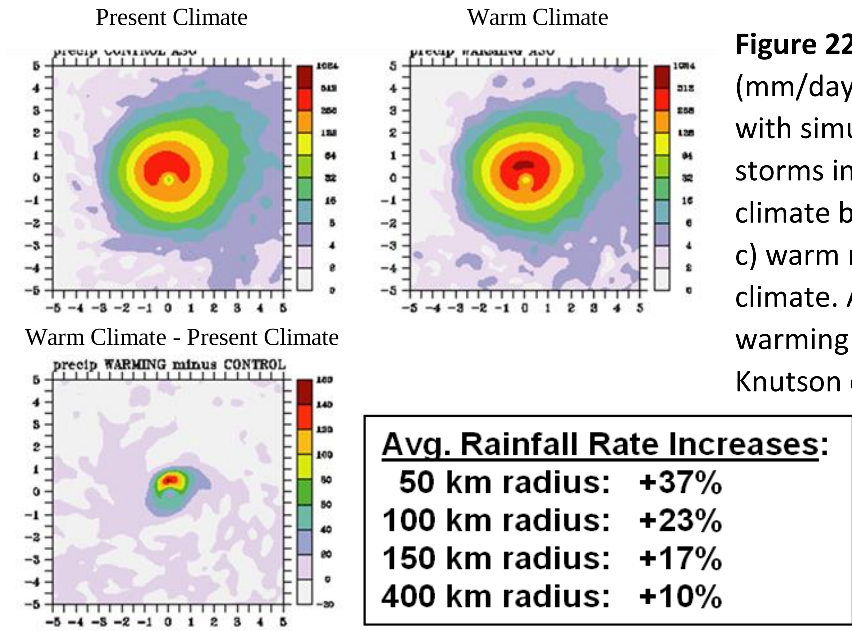

Figure 22: Rainfall rates (mm/day) associated with simulated tropical storms in a) a present climate b) warm climate c) warm minus present climate. Average warming is 1.72°C. From Knutson et al. (2010).

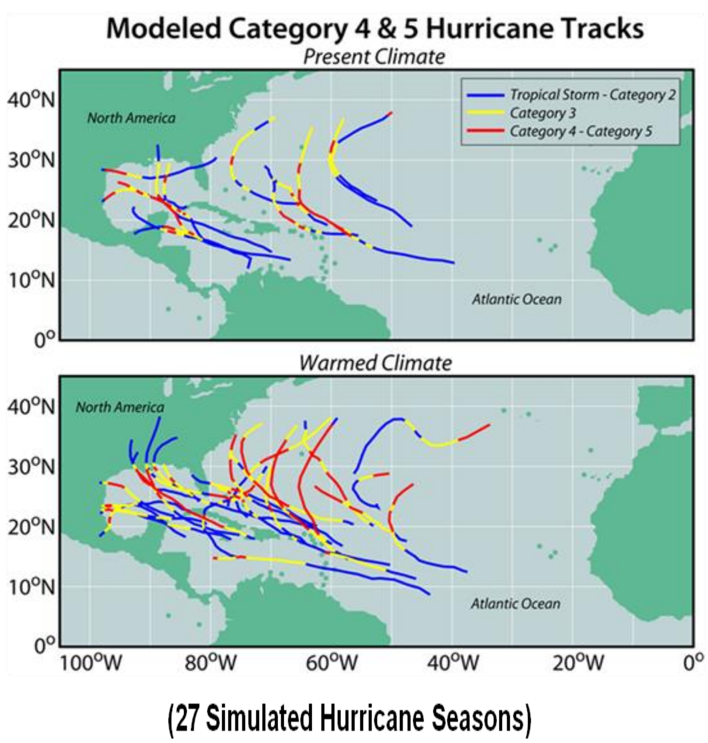

Figure 23: Late 21st century warming projections of category 4 and 5 hurricanes in the Atlantic. Average of 18 CMIP3 models. From Bender et al. (2010).

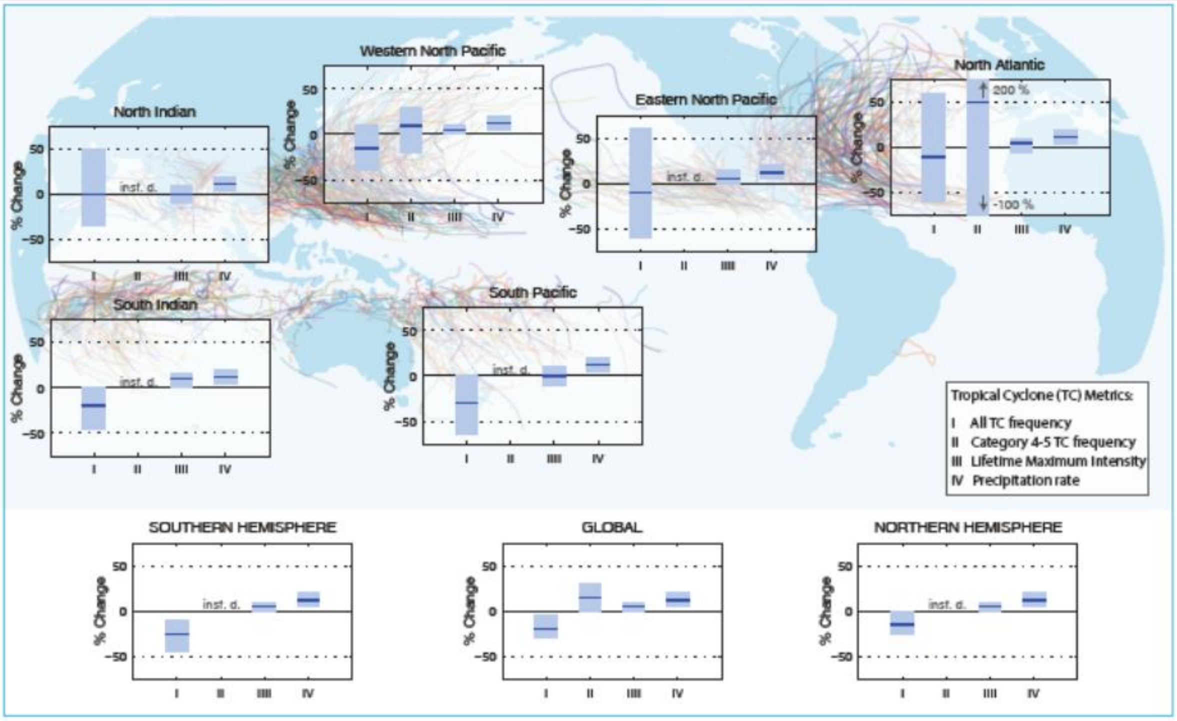

Figure 24: IPCC AR5 Summary Diagram

General consensus assessment of the numerical experiments described in IPCC (2013) Supplementary Material Tables 14.SM.1 to 14.SM.4. All values represent expected percent change in the average over period 2081–2100 relative to 2000–2019, under an A1B-like scenario, based on expert judgement after subjective normalization of the model projections. Four metrics were considered: the percent change in (I) the total annual frequency of tropical storms, (II) the annual frequency of Category 4 and 5 storms, (III) the mean Lifetime Maximum Intensity (LMI; the maximum intensity achieved during a storm's lifetime) and (IV) the precipitation rate within 200 km of storm centre at the time of LMI. For each metric plotted, the solid blue line is the best guess of the expected percent change, and the coloured bar provides the 67% (likely) confidence interval for this value (note that this interval ranges across –100% to +200% for the annual frequency of Category 4 and 5 storms in the North Atlantic). Where a metric is not plotted, there are insufficient data (denoted 'insf. d.') available to complete an assessment. A randomly drawn (and coloured) selection of historical storm tracks are underlain to identify regions of tropical cyclone activity.

7 Sea Levels

7.1 Current and Historical Trends

7.1.1 Globe

It is estimated that between 1901-2010 global mean sea level rose by 0.19 ± 0.02 m (IPCC 2013). Table 34 indicates the rates of increase in sea levels per year by data type.

Table 34: Mean rate of global averaged sea level rise

Period	Rate (mm/year)		Information source
1901 and 2010	1.7 ± 0.2	Tide gauge	IPCC (2013)
1993 and 2010	3.2 ± 0.4	Satellite Altimeter	IPCC (2013)

7.1.2 Caribbean

Rates of sea-level rise (SLR) are not uniform across the globe and large regional differences exist. Estimates of observed sea level rise from 1950 to 2000 suggest that sea level rise within the Caribbean appears to be near the global mean (Church et al. 2004).

Table 35: Mean rate of sea level rise averaged over the Caribbean basin.

Period	Rate (mm/year)	Information source
1950 and 2009	1.8 ± 0.1	Palanisamy et al. (2012)
1993 and 2010	1.7 ± 1.3	Torres and TSimplis (2013)
1993 and 2010	2.5± 1.3	Torres and TSimplis (2013), after correction for Global Isostatic Adjustment (GIA)

*GIA describes the slow part of the response of the earth to the redistribution of mass following the last deglaciation.

Figure 25 shows the general trend of sea level rise across the Caribbean region (Torres and TSimplis 2014). The tide gauge coverage in the Caribbean islands is poor with only 7 gauges having data greater than 30 years between 1950 and 2009. All values suggest an upward trend for the period of record available.

Inter-annual sea-level variability accounts for one third of the total sea-level variability and can be partly explained by the influence of El Nino-Southern Oscillation at different time and spatial scales (Palanisamy et al. 2013; Torres and Tsimplis 2014). Palanisamy et al. (2013) observe that inter-annual sea-level variability in the north Caribbean is higher than for the southern Caribbean and strongly correlated with El Niño.

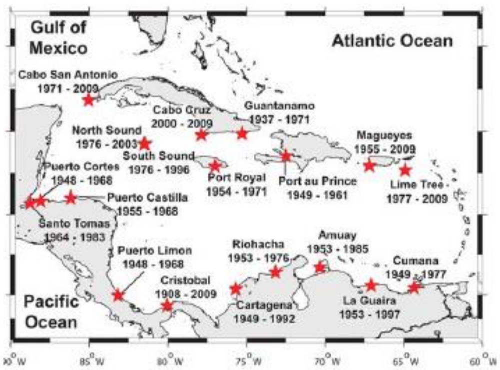

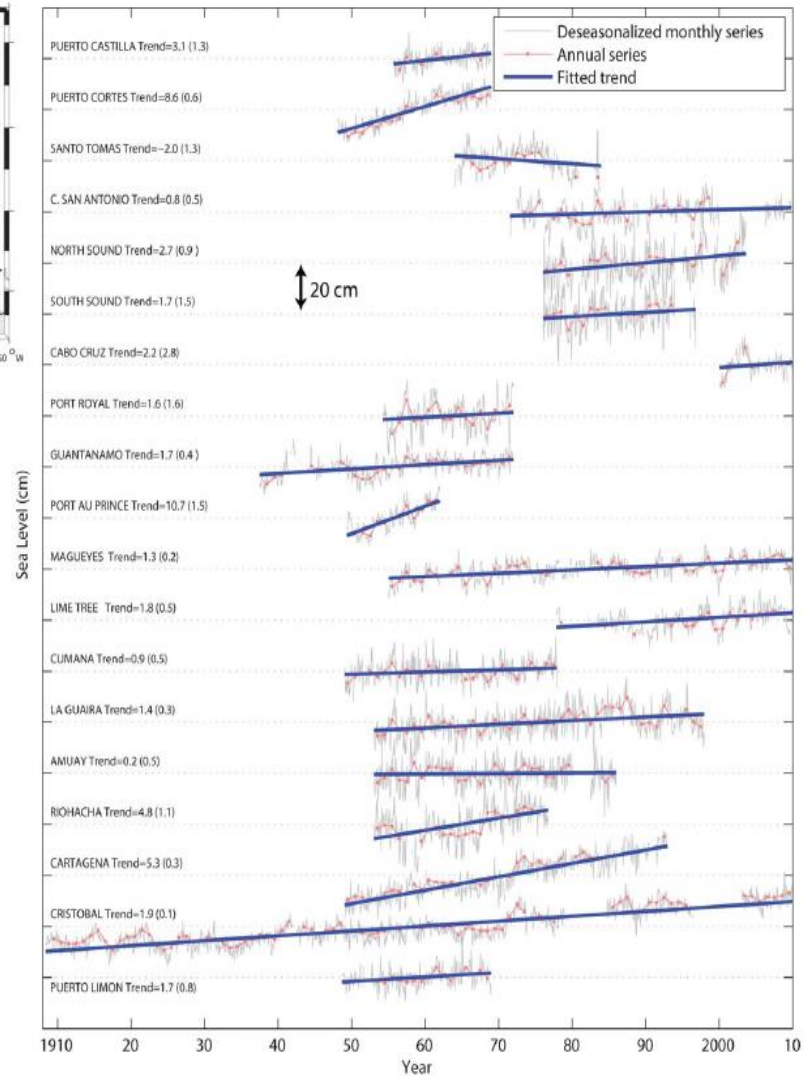

Figure 25: a) Location of tide gauge stations and time series start and end year. b) Tide gauge observed sea-level trends computed from all available data. Monthly time series after the removal of the seasonal cycle (gray), the linear trend (blue), and the annual series (red) are also shown. The trends (and 95% error) in mm/yr. From Torres and Tsimplis (2013).

7.1.3 The Bahamas

Sea level observations off the coast of Settlement Point, Grand Bahama, show significant increases in sea levels from 1985 to 2014 with a rate of increase of 0.0038 mm/month (Figure

26). Mean sea level observations as far back as 1983 at Vaca Key, Florida Bay, and Virginia Key (close in proximity to the northwest-most islands of The Abacos and Grand Bahama) indicate a rate of increase of 3.5 ± 0.01 mm/year (Park and Sweet 2015).

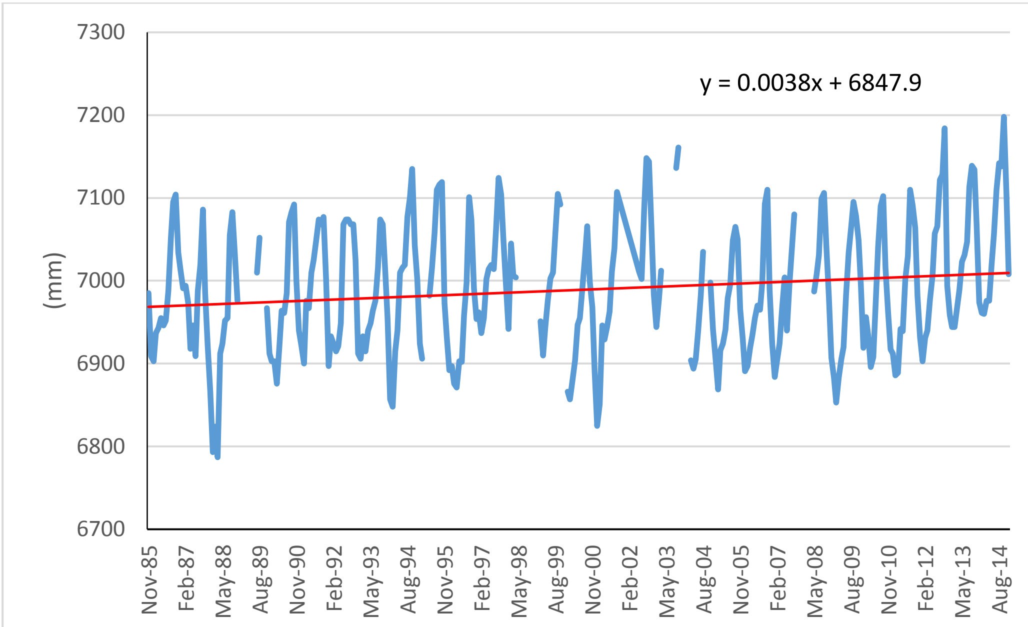

Figure 26: Monthly sea levels in millimeters at Settlement Point, Grand Bahama from 1985 to 2014. The red linear trend line indicates a rate of increase in sea levels of 0.0038mm/month. Data Source: PSMSL.

7.2 Projections

7.2.1 The Caribbean

Table 36 provides a range of estimates for end-of-century sea level rise globally and in the Caribbean Sea under a number of scenarios. The values are taken from the IPCC's Fourth Assessment Report. The future rise in the Caribbean is not significantly different from the projected global rise.

The combined range over all scenarios spans 0.18-0.59 m by 2100 relative to 1980-1999 levels. A number of other studies (e.g. Rahmstorf 2007; Rignot and Kanargaratnam 2006; Horton et al. 2008) including the recently released Summary of the Fifth Assessment Report (IPCC 2013) suggest that the upper bound for the global estimates in Table 32 are conservative and could be up to 0.98 m, with a rate during 2081–2100 of 8 to16 mm/ year. Diagrams from Perrette et al.

(2013) suggest the same for estimates for the Caribbean Sea i.e. a higher upper bound of up to 1.5 m by the end of the century.

Table 36: Projected changes in temperature per grid box by 2090s from a regional climate model

Scenario	Global Mean Sea Level Rise by 2100 relative to 1980 – 1999	Caribbean Mean Sea Level Rise by 2100 relative to 1980 – 1999 (± 0.05m relative to global mean)
IPCC B1	0.18 – 0.38	0.13 – 0.43
IPCC A1B	0.21 – 0.48	0.16 – 0.53
IPCC A2	0.23 – 0.51	0.18 – 0.56
Rahmstorf, 2007	Up to 1.4m	Up to 1.45 m
Perrette et al., 2013		Up to 1.50 m

The AR5 does not provide projections for the Caribbean separate from that for the Global mean. Nonetheless, the same assumption of SLR being similar for the region as for the globe is taken. Projections for the globe under the four RCPs are provided in Table 33. Through the mid-century, the mean increase is similar for all RCPs. Distinctions arise toward the end of the century. See also Figure 27.

Table 37: Projected increases in global mean sea level (m). Projections are taken from IPCC (2013) and are relative to 1986-2005.

		2046 – 2065		**2081– 2100**	
Variable	Scenario	Mean	Likely range	Mean	Likely range
Global Mean Sea Level Rise (m)	RCP2.6	0.24	0.17 – 0.32	0.40	0.26 – 0.55
	RCP4.5	0.26	0.19 – 0.33	0.47	0.32 – 0.63
	RCP6.0	0.25	0.18 – 0.32	0.48	0.33 – 0.63
	RCP8.5	0.30	0.22 – 0.38	0.63	0.45 – 0.82

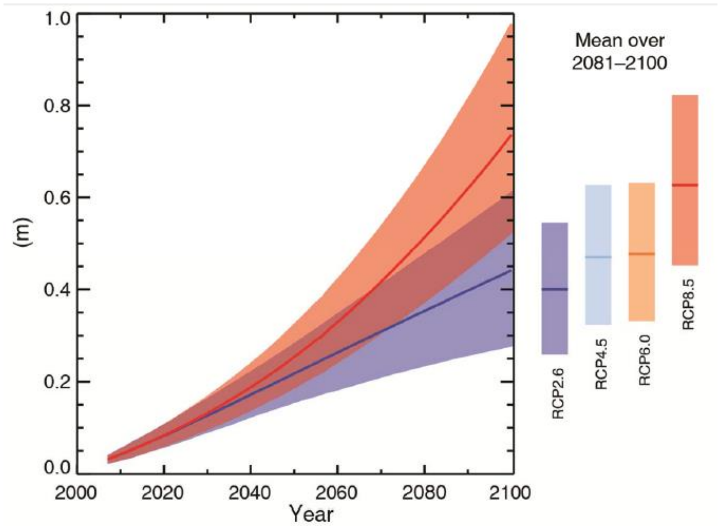

Figure 27: Projections of global mean sea level rise over the 21st century relative to 1986–2005 from the combination of the CMIP5 ensemble with process-based models, for RCP2.6 and RCP8.5. The assessed *likely* range is shown as a shaded band. The assessed *likely* ranges for the mean over the period 2081–2100 for all RCP scenarios are given as coloured vertical bars, with the corresponding median value given as a horizontal line. From IPCC (2013)

7.2.2 The Bahamas

Projections indicate that the eastern most coasts of The Bahamian Isles expect to see a marginally slower rate of increase compared to the western most coasts. Table 34 highlights the steady increase in mean sea level rise for the four RCP scenarios. The eastern and western-most coasts show a similar range of sea level increases across the time slices with a general difference of 0.01-0.02m between trends. Figure 28 also shows an increase in sea level rise under low, medium and high sensitivity conditions, with a greater rate of increase under the RCP8.5 scenario.

Table 38: Projected increases in mean sea level rise (m) for the east and west coasts of The Bahamas. Range is the lowest projection under low sensitivity conditions to the highest annual projection under high sensitivity during the period. Projections relative to 1986-2005.

	Sea Level Rise (m) East Coast (-77.076W, 18.8605N)							
Centered on	**2025**		**2035**		**2055**		**End of century**	
Averaged over	**2016-2035**		**2026-2045**		**2046-2065**		**2081-2100**	
	Mean	**Range**	**Mean**	**Range**	**Mean**	**Range**	**Mean**	**Range**
RCP2.6	0.11	0.05 – 0.20	0.16	0.08 – 0.27	0.26	0.15 – 0.41	0.44	0.26 – 0.67
RCP4.5	0.10	0.05 – 0.20	0.16	0.08 – 0.26	0.28	0.16 – 0.43	0.52	0.32 – 0.78
RCP6.0	0.10	0.05 – 0.19	0.15	0.08 – 0.25	0.27	0.15 – 0.42	0.53	0.32 – 0.80
RCP8.5	0.11	0.05 – 0.21	0.17	0.08 – 0.30	0.32	0.18 – 0.52	0.70	0.42 – 1.09
	Sea Level Rise (m) West Coast (-77.157W, 17.142N)							
Centered on	**2025**		**2035**		**2055**		**End of century**	
Averaged over	**2016-2035**		**2026-2045**		**2046-2065**		**2081-2100**	
	Mean	**Range**	**Mean**	**Range**	**Mean**	**Range**	**Mean**	**Range**
RCP2.6	0.11	0.05 – 0.20	0.16	0.08 – 0.27	0.27	0.15 – 0.42	0.46	0.27 – 0.69
RCP4.5	0.11	0.05 – 0.20	0.16	0.08 – 0.27	0.29	0.17 – 0.45	0.54	0.33 – 0.81
RCP6.0	0.11	0.05 – 0.19	0.16	0.08 – 0.26	0.28	0.15 – 0.43	0.54	0.33 – 0.83
RCP8.5	0.11	0.05 – 0.21	0.18	0.08 – 0.31	0.33	0.19 – 0.54	0.72	0.43 – 1.12

a)

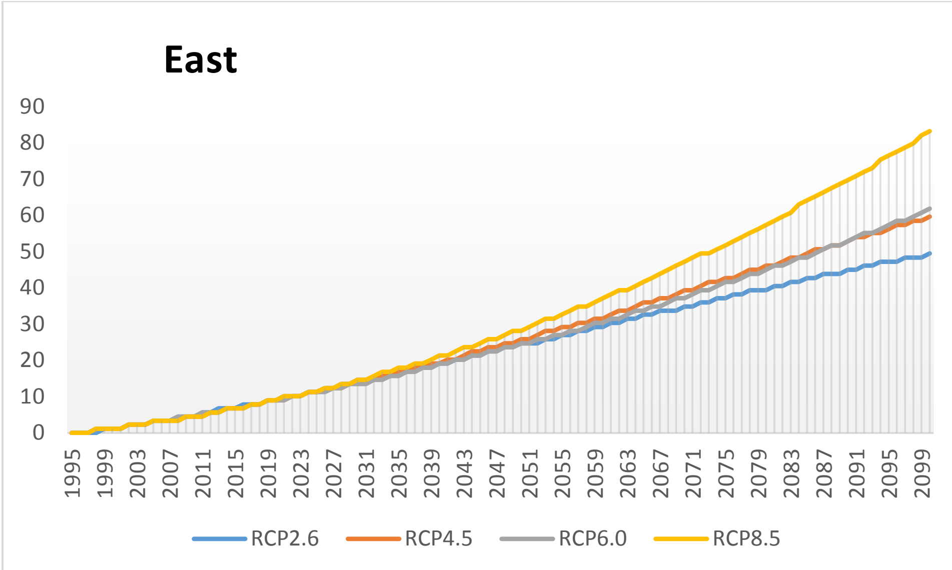

b)

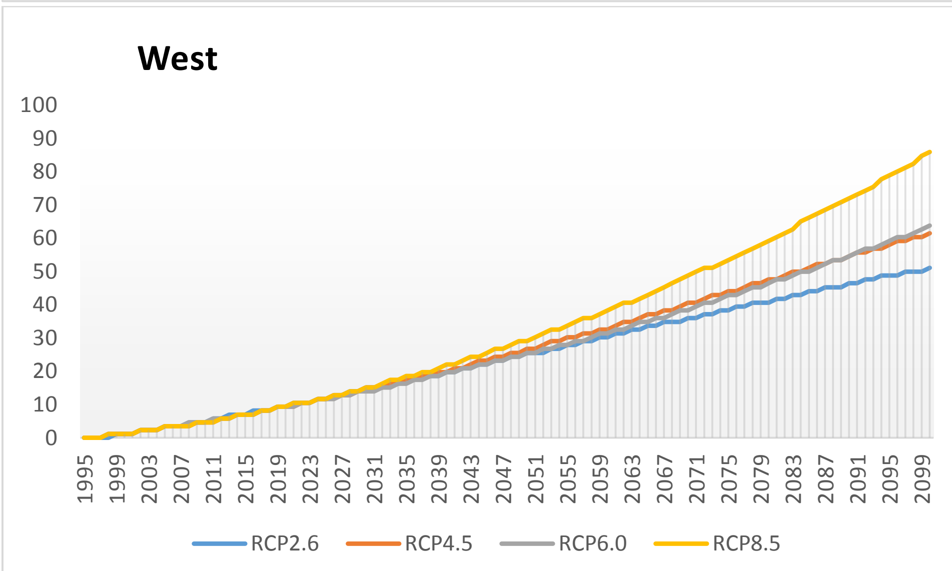

Figure 28: Sea level rise projections under RCP2.6, RCP4.5, RCP6.0 and RCP8.5 for a) a point (-77.08°W, 18.86°N) off the Eastern region of the Bahamas; b) a point (-77.16°W, 17.14°N) off the Western region of the Bahamas.

7.3 Sea Level Extremes

Adapted from IPCC (2013)

Higher mean sea levels (MSL) can significantly decrease the return period for exceeding given threshold levels. Hunter (2012) determined the factor by which the frequency of sea levels exceeding a given height would be increased for a mean sea level rise of 0.5 m for a network of 198 tide gauges covering much of the globe (Figure 30). The AR5 repeats the calculations using regional sea level projections and their uncertainty under the RCP4.5 scenario. The multiplication factor depends exponentially on the inverse of the Gumbel scale parameter (a factor which describes the statistics of sea level extremes caused by the combination of tides and storm surges) (Coles and Tawn, 1990). The scale parameter is generally large where tides and/or storm surges are large, leading to a small multiplication factor, and vice versa. Figure 29 shows that a 0.5 m MSL rise would *likely* result in the frequency of sea level extremes increasing by an order of magnitude or more in some regions. The multiplication factors are found to be slightly higher, in general, when accounting for regional MSL projections. In regions having higher regional projections of mean sea level the multiplication factor is higher, whereas in regions having lower regional projections of mean sea level the multiplication factor is lower.

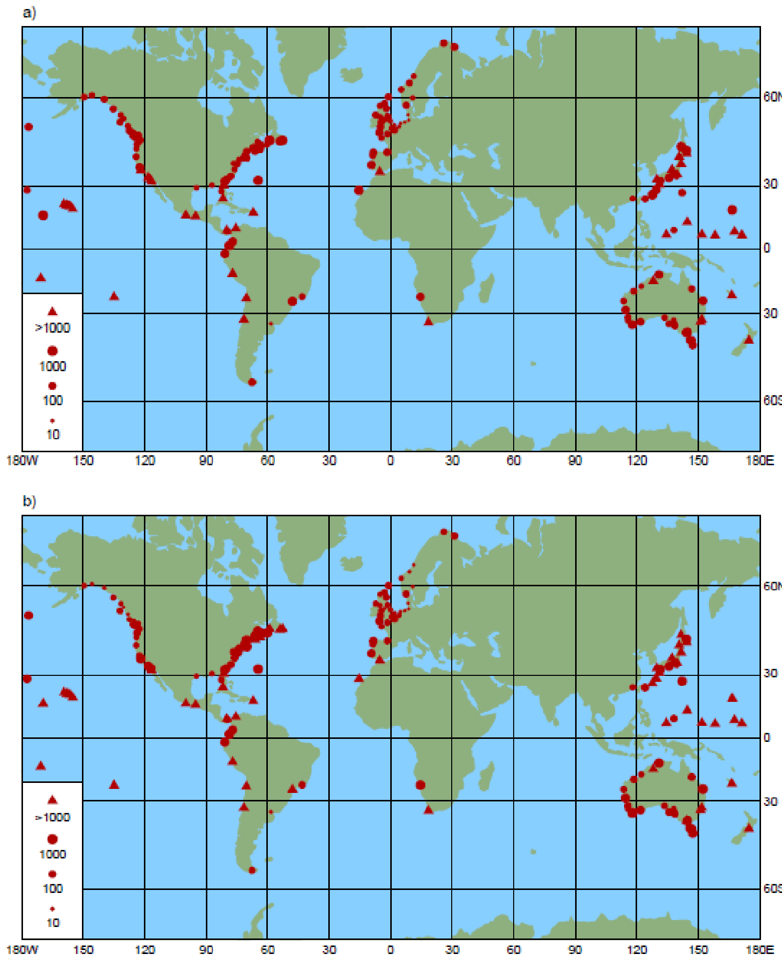

Figure 29: The estimated multiplication factor (shown at tide gauge locations by red circles and triangles), by which the frequency of flooding events of a given height increase for (a) a mean sea level rise of 0.5 m (b) using regional projections of mean se level for the RCP4.5 scenario. The Gumbel scale parameters are generally large in regions of large tides and/or surges resulting in a small multiplication factor and vice versa. IPCC (2013)

8 References

Antuña-Marrero, J.C., O.H. Otterå, A. Robock, and M.D. Mesquita. 2015. "Modelled and observed sea surface temperature trends for the Caribbean and Antilles." *International Journal of Climatology* 36(4): 1873-1886. doi: 10.1002/joc.4466.

Bender, M.A., T.R. Knutson, and R.E. Tuleya. 2010. "Modeled impact of anthropogenic warming on the frequency of intense Atlantic hurricanes." *Science* 327(5964): 454–458. http://www.ncbi.nlm.nih.gov/pubmed/20093471.

Campbell, J.D., M.A. Taylor, T.S. Stephenson, R.A. Watson, and F.S. Whyte. 2011. "Future climate of the Caribbean from a regional climate model." *International Journal of Climatology* 31(12): 1866–1878.

Chenoweth, M. 1998. "The early 19th century climate of the Bahamas and a comparison with 20th century averages." *Climatic Change* 40(3-4): 577-603.

Chu, P-S. 2004. "ENSO and tropical cyclone activity." *Hurricanes and typhoons: Past, present, and potential*, 297-332.

Church, J.A., N.J. White, R. Coleman, K. Lambeck, and J.X. Mitrovica. 2004. "Estimates of the regional distribution of sea level rise over the 1950-2000 period." *Journal of climate* 17(13): 2609-2625.

Coles, S.G., and J.A. Tawn. 1990. "Statistics of coastal flood prevention." *Philosophical Transactions of the Royal Society of London A: Mathematical, Physical and Engineering Sciences* 332 (1627): 457-476.

Emanuel, K. 2007. "Environmental factors affecting tropical cyclone power dissipation." *Journal of Climate*, 20(22), pp.5497–5509. http://journals.ametsoc.org/doi/abs/10.1175/2007JCLI1571.1.

Gamble, D.W., and S. Curtis. 2008. "Caribbean precipitation: review, model and prospect." *Progress in Physical Geography*, 32(3): 265–276.

Giannini, A., Y. Kushnir, M.A. Cane. 2000. "Interannual variability of Caribbean rainfall, ENSO, and the Atlantic Ocean." *Journal of Climate* 13: 297-311.

Giannini, A., T. Kushnir, and M.A. Cane. 2001. "Seasonality in the impact of ENSO and the North Atlantic High on Caribbean rainfall." *Physics and Chemistry of the Earth (B)* 26(2): 143-147.

Goldenberg, S.B., C.W. Landsea, A.M. Mestz-Nuñez, and W.M. Gray. 2001. "The recent increase in Atlantic hurricane activity: Causes and implications." *Science* 293(5529): 474–479. http://www.sciencemag.org/content/293/5529/474.short.

Horton, R., C. Herweijer, C. Rosenzweig, J. Liu, V. Gornitz and A.C. Ruane. 2008. "Sea level rise projections for current generation CGCMs based on the semi-empirical method" *Geophysical Research Letters,* 35, L02715.

Hunter, J. 2012. "A simple technique for estimating an allowance for uncertain sea-level rise." *Climatic Change* 113 (2): 239-252.

IPCC. 2012. "Managing the Risks of Extreme Events and Disasters to Advance Climate Change Adaptation. A Special Report of Working Groups I and II of the Intergovernmental Panel on Climate Change" [Field, C.B., V. Barros, T.F. Stocker, D. Qin, D.J. Dokken, K.L. Ebi, M.D. Mastrandrea, K.J. Mach, G.-K. Plattner, S.K. Allen, M. Tignor, and P.M. Midgley (eds.)]. Cambridge University Press, Cambridge, UK, and New York, NY, USA, 582 pp

IPCC. 2013. "Climate Change 2013: The Physical Science Basis. Contribution of Working Group I to the Fifth Assessment Report of the Intergovernmental Panel on Climate Change" [Stocker, T.F., D. Qin, G.-K. Plattner, M. Tignor, S.K. Allen, J. Boschung, A. Nauels, Y. Xia, V. Bex and P.M. Midgley (eds.)]. Cambridge University Press, Cambridge, United Kingdom and New York, NY, USA, 1535 pp, doi:10.1017/CBO9781107415324.

Jones, R. G., M. Noguer, D. Hassell, D. Hudson, S. Wilson, G. Jenkins, and J. Mitchell. 2003. "Workbook on generating high resolution climate change scenarios using PRECIS. UNDP, GEF, and Met Office Hadley Centre Manual." 32 pp.

Klotzbach, P.J. 2007. "Recent developments in statistical prediction of seasonal Atlantic basin tropical cyclone activity." *Tellus A* 59 (4): 511-518.

Klotzbach, P.J., 2011. "A simplified Atlantic basin seasonal hurricane prediction scheme from 1 August." *Geophysical Research Letters*, 38(16):1–4.

Knutson, T.R., J.L. McBride, J. Chan, K. Emanuel, G. Holland, C. Landsea, I. Held, J.P. Kossin, A.K. Srivastava, and M. Sugi. 2010. "Tropical cyclones and climate change." *Nature Geoscience* 3: 157-163. doi:10.1038/ngeo779.

Knutson, Thomas R., J.J. Sirutis, G.A. Vecchi, S. Garner, M. Zhao, H.-S. Kim, M. Bender, et al. 2013. "Dynamical Downscaling Projections of Twenty-First-Century Atlantic Hurricane Activity: CMIP3 and CMIP5 Model-Based Scenarios." *Journal of Climate* 26: 6591–6617. doi: http://dx.doi.org/10.1175/JCLI-D-12-00539.1

Magaña, V., J.A. Amador, and S. Medina. 1999. "The midsummer drought over Mexico and Central America." *Journal of Climate* 12(6): 1577–1588.

Maldonado, T., A. Rutgersson, J. Amador, E. Alfaro, and B. Claremar. 2015. "Variability of the Caribbean low-level jet during boreal winter: large-scale forcings." *International Journal of Climatology* 36 (4): 1954-1969.

McSweeney, C., M. New, G. Lizcano, and X. Lu. 2010. "The UNDP Climate Change Country Profiles Improving the Accessibility of Observed and Projected Climate Information for Studies of Climate Change in Developing Countries." *Bulletin of the American Meteorological Society* 91: 157-166.

Nakićenović, N., and R. Swart (eds.). 2000. "Special Report on Emissions Scenarios. A Special Report of Working Group III of the Intergovernmental Panel on Climate Change." Cambridge University Press, Cambridge, United Kingdom and New York, NY, USA, 599 pp.

Palanisamy, H., M. Becker, B. Meyssignac, O. Henry, and A. Cazenave. 2012. "Regional sea level change and variability in the Caribbean sea since 1950." *Journal of Geodetic Science* 2(2): 125-133.

Park, J., and W. Sweet. 2015. "Accelerated sea level rise and Florida Current transport." *Ocean Science* 11 (4): 607-615.

Perrette, M., F. Launderer, R. Riva, K. Frieler, and M. Meinshausen. 2013. "A scaling approach to project regional sea level rise and its uncertainties." *Earth Syst. Dynam*. 4: 11–29.

Rahmstorf, S. 2007. "A semi-empirical approach to projecting future sea level rise." *Science* 315 (5810): 368-370.

Rignot, E. and P. Kanagaratnam. 2006. "Changes in the velocity structure of the Greenland Ice Sheet." *Science* 311(5763): 986-990.

Stephenson, T.S. L.A. Vincent, T. Allen, C.J. van Meerbeeck, M. McLean, T.C. Peterson, M.A. Taylor, et al. 2014. "Changes in extreme temperature and precipitation in the Caribbean region, 1961–2010." *International Journal of Climatology* 34(9): 2957–2971.

Taylor, M.A., D.B. Enfield, and A.A. Chen. 2002. "Influence of the tropical Atlantic versus the tropical Pacific on Caribbean rainfall." *Journal of Geophysical Research* 107(C9): 3127.

Taylor, M.A., A. Centella, J. Charlery, A. Bezanilla, J. Campbell, I. Borrajero, T.S. Stephenson, and R. Nurmohamed. 2013. "The precis Caribbean story lessons and legacies." *Bulletin of the American Meteorological Society* 94(7): 1065–1073.

Torres, R.R., and M.N. Tsimplis. 2014. "Sea level extremes in the Caribbean Sea." *Journal of Geophysical Research: Oceans* 119 (8): 4714-4731.

Webster, P.J., G.J. Holland, J.A. Curry, and H.-R. Chang. 2005. "Changes in tropical cyclone number, duration, and intensity in a warming environment." *Science* 309(5742):1844–6.

9 Appendix

Tables A1 – A3: Annual projections of mean, minimum, and maximum temperature change and the percentage change in precipitation by grid box for the 2020's, 2030's, and 2050's.

Table A1: Great Exuma

Grid Box	2020's				2030's				2050's			
	Mean Temp(◦C)	Min Temp (◦C)	Max Temp (◦C)	Precip (%)	Mean Temp(◦C)	Min Temp (◦C)	Max Temp (◦C)	Precip (%)	Mean Temp(◦C)	Min Temp (◦C)	Max Temp (◦C)	Precip (%)
1	1.08	1.09	1.10	5.27	1.39	1.40	1.42	8.02	1.94	2.15	1.71	0.74
2	1.10	1.13	1.11	7.48	1.42	1.44	1.44	7.82	2.01	2.74	1.13	11.27
3	1.11	1.15	1.11	6.80	1.43	1.46	1.45	6.18	2.04	2.92	0.98	23.17

Table A2: Eleuthera

Grid Box	2020's				2030's				2050's			
	Mean Temp(◦C)	Min Temp (◦C)	Max Temp (◦C)	Precip (%)	Mean Temp(◦C)	Min Temp (◦C)	Max Temp (◦C)	Precip (%)	Mean Temp(◦C)	Min Temp (◦C)	Max Temp (◦C)	Precip (%)
4	1.17	1.26	1.15	6.37	1.46	1.53	1.44	1.43	2.13	2.27	2.05	3.79
5	1.21	1.30	1.18	3.44	1.49	1.58	1.48	-0.32	2.23	2.33	2.22	0.98
6	1.18	1.25	1.19	3.91	1.46	1.53	1.47	1.70	2.28	2.28	2.42	4.40
7	1.11	1.15	1.11	7.72	1.38	1.41	1.40	4.61	2.09	2.08	2.18	8.12
8	1.22	1.32	1.21	1.62	1.49	1.58	1.49	0.78	2.44	2.37	2.69	0.25
9	1.21	1.30	1.20	2.95	1.48	1.57	1.48	1.46	2.44	2.23	2.85	-2.09
10	1.21	1.31	1.19	3.89	1.48	1.57	1.48	1.35	2.47	2.10	3.10	-3.66

Table A3: Great Abaco

Grid Box	2020's				2030's				2050's			
	Mean Temp(◦C)	Min Temp (◦C)	Max Temp (◦C)	Precip (%)	Mean Temp(◦C)	Min Temp (◦C)	Max Temp (◦C)	Precip (%)	Mean Temp(◦C)	Min Temp (◦C)	Max Temp (◦C)	Precip (%)
11	1.14	1.19	1.15	3.36	1.41	1.46	1.41	1.32	2.22	2.22	2.33	2.19
12	1.18	1.24	1.18	3.32	1.44	1.51	1.44	1.04	2.28	2.66	1.89	11.79
13	1.19	1.26	1.19	3.28	1.45	1.53	1.44	1.98	2.36	2.39	2.46	7.65
14	1.19	1.26	1.19	3.33	1.45	1.52	1.45	0.76	2.32	2.50	2.20	13.31
15	1.18	1.25	1.19	3.37	1.44	1.51	1.44	1.59	2.32	2.31	2.47	8.93
16	1.17	1.24	1.17	3.67	1.43	1.49	1.43	0.65	2.29	1.87	3.00	4.44
17	1.19	1.26	1.20	3.07	1.44	1.51	1.44	0.92	2.34	2.06	2.85	2.94
18	1.17	1.23	1.18	1.28	1.41	1.48	1.41	-0.94	2.28	1.81	3.04	0.91
19	1.14	1.18	1.15	1.36	1.38	1.42	1.39	-2.49	2.18	1.79	2.80	-0.34
20	1.11	1.14	1.12	2.34	1.36	1.38	1.12	-2.22	2.10	2.07	2.19	1.94